vibration

MDPI

Review

Experimental Linear and Nonlinear Vibration Methods for the Structural Health Monitoring (SHM) of Polymer-Matrix Composites (PMCs): A Literature Review

Loan Dolbachian *, Walid Harizi and Zoheir Aboura

Centre de Recherche Royallieu, Roberval (Mechanics Energy and Electricity), Université de Technologie de Compiègne, CEDEX CS 60 319, 60 203 Compiègne, France; walid.harizi@utc.fr (W.H.); zoheir.aboura@utc.fr (Z.A.)
* Correspondence: loan.dolbachian@utc.fr

Abstract: The goal of this article is to provide a review of the experimental techniques and procedures using vibration methods for the Structural Health Monitoring (SHM) of Polymer-Matrix Composites (PMCs). It aims to be a guide for any researchers to carry out vibration experiments. The linear methods are first introduced. But, as PMC is a complex material, these classic methods show some limits, such as low accuracy for small damages and a high environmental dependency. This is why the nonlinear methods are secondly studied, considering that the complexity of PMCs induces a nonlinear behavior of the structure after damage occurrence. The different damage mechanisms are well-explained in order to evaluate the potential of each vibration method to detect them.

Keywords: Polymer-Matrix Composites (PMC); Structural Health Monitoring (SHM); vibration analysis; linear/nonlinear methods

Citation: Dolbachian, L.; Harizi, W.; Aboura, Z. Experimental Linear and Nonlinear Vibration Methods for the Structural Health Monitoring (SHM) of Polymer-Matrix Composites (PMCs): A Literature Review. *Vibration* **2024**, *7*, 281–325. https://doi.org/10.3390/vibration7010015

Academic Editors: Francesco Pellicano, Yuri Mikhlin, Konstantin V. Avramov and Antonio Zippo

Received: 31 January 2024
Revised: 5 March 2024
Accepted: 8 March 2024
Published: 12 March 2024

1. Introduction

Nowadays, the use of PMCs in industrial sectors, such as aeronautics and the automotive sector, is sharply increasing thanks to their high mechanical properties, low weight, high resistance to corrosion environments, etc. [1–10], permitting them to challenge classical materials like metals. Table 1 references some mechanical characteristics of three different types of PMCs in comparison with two classical materials, steel and aluminum. The key synthetic parameters used to assess the mechanical performance of a composite include the specific modulus (the ratio of elasticity modulus to density E/ρ) and the specific strength (the ratio of ultimate strength to density R_e/ρ). Typically, these properties are governed by the fibers. When comparing mechanical properties with mass considerations, the three PMC materials seem to offer more promise than the two metallic materials. In recent years, there has been a significant increase in the number of articles published about PMCs (Figure 1), with a surge starting around 2010. PMCs are made of fiber and matrix. The combination and variation of the fraction or orientation of fibers make it a complex, heterogeneous, and anisotropic material, which complicates its damage mechanisms. This is why measuring and understanding them as well as evaluating their impact on the structure are important to ensure the continuity of services. This is known as Structural Health Monitoring (SHM). The concept of SHM brought these four steps [11]: (i) detect damage in the structure; (ii) localize it; (iii) quantify its severity and qualify it; and (iv) give a conclusion regarding the service life of the structure. This review mainly explores the first two steps of SHM by focusing on the methods used and does not cover the prognostic part.

Table 1. Absolute and reduced characteristics of three PMCs and two metals [12].

Material	Volume Mass ρ (g/cm^3)	Young's Modulus E (GPa)	Strength R_e (MPa)	Tenacity K_{IC} (MPam$^{1/2}$)	E/ρ	$E^{1/2}/\rho$	$E^{1/3}/\rho$	R_e/ρ
Composite								
Carbon-Fiber-Reinforced Polymer (58% uniaxial fiber in epoxy)	1.5	189	1050	32–45	126	9	3.8	700
Glass-Fiber-Reinforced Polymer (50% uniaxial fiber in epoxy)	2.0	48	1240	42–60	24	3.5	1.8	620
Kevlar-Fiber-Reinforced Polymer (60% uniaxial fiber in epoxy)	1.4	79	1240	-	54	6.2	3.0	886
Metal								
High-resistance steel	7.8	207	1000	100	27	1.8	0.76	128
Aluminum alloy	2.8	71	500	28	25	3.0	1.5	179

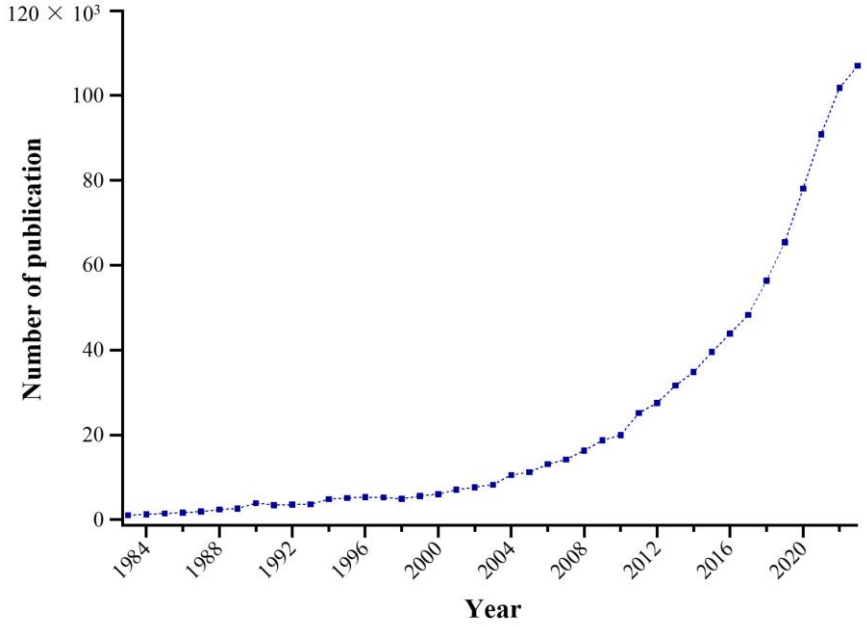

Figure 1. Number of articles published during the past 40 years about PMC. (source = https://app.dimensions.ai/discover/publication, accessed on 6 March 2024).

Many Non-Destructive Testing (NDT) techniques are available for SHM purposes [13], such as Ultrasonic Testing (UT) [14,15], Acoustic Emission (AE) [16,17], Digital Image Correlation (DIC) [18,19], X-ray tomography [20,21], Infrared thermography [22], Vibration analysis [23], and others. In the literature, many reviews have focused on the numerical aspects of vibration analysis and/or do not distinguish the type of material. Given the growing utilization of PMC materials and their complex behavior, it is necessary to understand how they vibrate and what influences the damage mechanisms have on the vibration.

The vibration of a structure provides a wealth of information regarding its physical properties, which motivates its use as a damage indicator [24–31]. Indeed, the vibration of a system follows the equation of motion of a forced-damped system:

$$m\ddot{x} + c\dot{x} + kx = F(t) \quad (1)$$

where $\ddot{x}$, $\dot{x}$ represent the second and first time-derivatives of the displacement x, m is the mass, c is the viscous coefficient, k is the stiffness of the system, and $F(t)$ is an external force applied to the system as a function of time. The vibration parameters, such as natural

frequency (f_0) or damping ratio (ζ), can be calculated from this formula and clearly show that a change in the material characteristics due to damage will influence the vibration:

$$\ddot{x} + 2\zeta\dot{x} + {\omega_0}^2 x = \frac{F(t)}{m}$$
$$\zeta = \frac{c}{2\sqrt{mk}} \qquad f_0 = 2\pi\omega_0 = 2\pi\sqrt{\frac{k}{m}} \tag{2}$$

The vibration methods for SHM are divided into two parts: the linear and the nonlinear methods. Linear vibration methods have been known and utilized for a long time, but innovations in their application still represent a current field of research. On the other hand, nonlinear methods have shown increasing interest from the 2010s to the present day. Given the anisotropy and the heterogeneous aspects of PMCs, it turns out that the detection and quantification of their damage mechanisms are more relevant using nonlinear vibration methods [32]. Considering that, it is worthwhile to undertake a review that highlights the greater effectiveness of the nonlinear methods over the linear ones for PMC material while still introducing both approaches. As it aims to be a guide to the different experimental vibration methods, the equipment, the devices used for each method, and the damages studied in the literature will be described in detail.

This article is divided as follows. The first part introduces the PMCs: their composition, the different kinds of architecture, and the principal damage mechanisms that can occur. The second part describes the methods and the equipment used in the literature. The third part is the main part of this review, and it introduces the experimental linear and nonlinear vibration analyses and the damage specificities.

2. Reminder about PMCs and Their Damage Mechanisms

A composite is a structural material that combines two different components. One is the matrix and the other is the reinforcement. There exist several types of composites depending on the used constituents: the Ceramic-Matrix Composites (CMCs), the Metal-Matrix Composites (MMCs), and the PMCs. As their application domains are different, this article only focuses on the PMC, which is a material of wide diffusion.

2.1. Composition and Structure of PMC

In PMC, the reinforcing part is made of continuous or short fibers and the matrix is made of polymers, such as thermoplastic or thermoset resins [6,33]. The volume or the orientation of the fibers, the number of layers, the different possible structures, and the different possible constituents expand the possibilities in the creation of PMC. A list of possible constituents of PMCs is given in Table 2.

Table 2. PMC composition.

Reinforcement (Fiber)	**Matrix (Polymer)**	
	Thermoplastics	**Thermosets**
Carbon Glass Aramid (Kevlar) Polypropylene Hemp Flax etc.	Nylon Polypropylene Polycarbonate Cellulose Acetate Polystyrene Polyethylene Polyvinyl chloride Acrylonitrile-butadiene-styrene Polyether-ether-ketone etc.	Phenolic Polyimide Polyurethane Polyepoxide Polyester etc.

Due to the polymer resin, which can dissipate energy through internal friction and molecular relaxation processes [34], a PMC exhibits a viscoelastic behavior that significantly

influences vibration analysis. This viscoelasticity can be characterized through dynamic mechanical analysis, which involves the application of a small oscillatory stress to the material while measuring the strain resulting from this load. The stress σ and the strain ε can then be linked with a dynamic modulus G:

$$\sigma = G\,\varepsilon \qquad\qquad G = G' + iG'' \tag{3}$$

where G' is the storage modulus representing the elastic behavior and G'' is the loss modulus representing the viscous behavior. The phase angle δ represents the combination of viscous and elastic behavior within the material and will be included between 0 and 90° ($\delta = 0°$ indicates purely elastic behavior (energy stored and restituted by the material) and $\delta = 90°$ indicates purely viscous behavior (energy dissipated in the form of heat)):

$$\tan\,\delta = \frac{G''}{G'} \tag{4}$$

The common structures made of PMC are the laminates and the sandwiches, both of which are shown in Figure 2. The laminated composite consists of the assembly of several plies with different fiber orientations, while the sandwich is made of two thin skins joined with an adhesive to a core; the skin is made of laminates and the core is made of a thick, low-strength material that can be foam material, such as polyurethane, honeycombs, and others. The layers of laminates can either be made of unidirectional, short, or woven fibers [35]. The woven fabric consists of the interlacing of warp and weft fibers with a specific pattern (plain, satin, twill, etc.) (Figure 3).

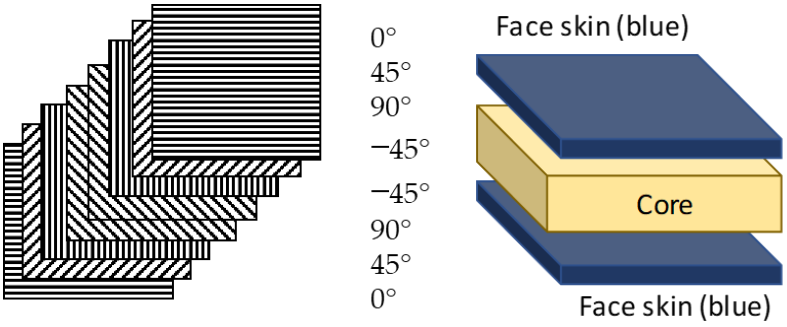

Figure 2. Laminated (**left**) and sandwich composite (**right**).

Recently, many 3D woven composites have been developed for particular applications (aerospace and defense domains), and some studies of their mechanical properties have been proposed [36].

2.2. Damage Mechanisms

In a PMC's service life, four main damage mechanisms can cause structure failure: matrix cracking, fiber breaking, delamination, and fiber–matrix interfacial debonding. They can be observed in Figure 4 coming from an impact. Many articles have used impact damage in their research, including, mainly, the BVID (Barely Visible Impact Damage) [37], which is a common way of introducing damage within PMC materials through low-velocity impact. The damage introduced through BVID could be a mix of the four main damage mechanisms while varying based on the architecture and composition of the PMC structure. In general, damage starts with very small matrix cracking (microcracks) and the three other mechanisms will be induced from this start, resulting in a combination of them. On a laboratory scale, these damages can be artificially generated: fiber-breakage can be made from fiber cutting before the manufacturing step, delamination can be introduced by inserting Teflon or foreign film between two plies, etc. In service, impact damage is common, and it results in the same damage mechanisms. The more forceful the impact, the more the structure is damaged. In reference [38], a clarification is made regarding the

characteristic failure mechanisms of PMC. In Figure 5, we can observe the evolution of damages during a tensile test.

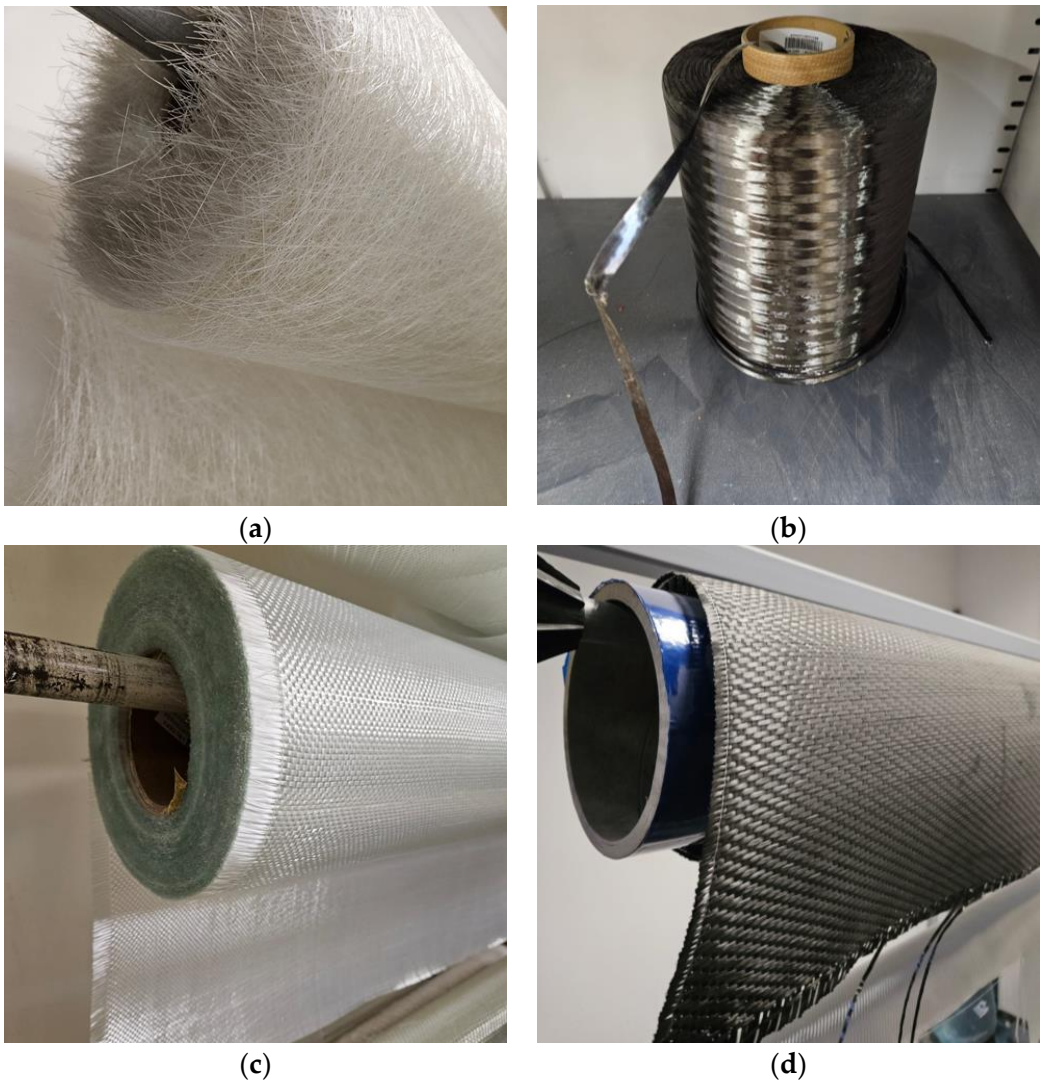

Figure 3. Different architectures of fibers: (**a**) mat short glass fiber, (**b**) continuous carbon fiber, (**c**) plain glass fiber, and (**d**) twill 2/1 carbon fiber.

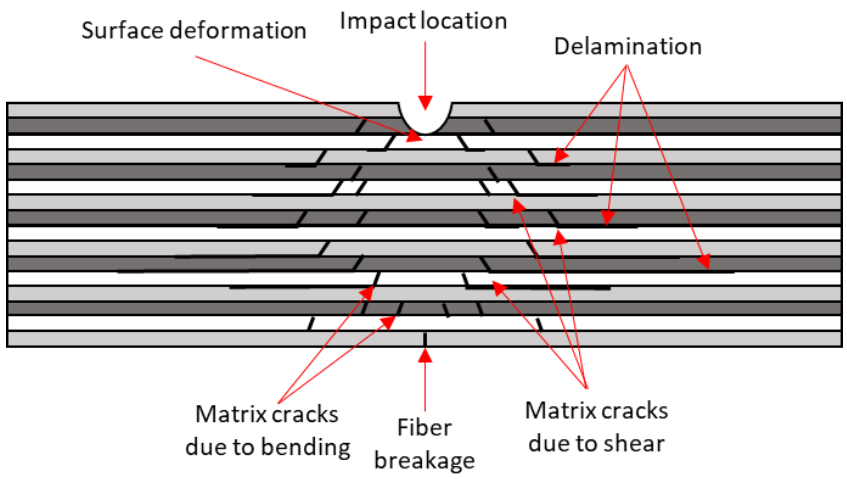

Figure 4. Impact damage mechanisms in composite laminate (adapted from [39]).

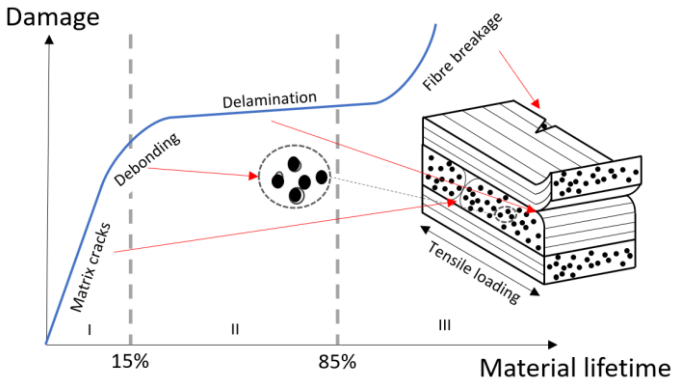

Figure 5. Evolution of damage in composite laminate (adapted from [40]).

2.2.1. Matrix Cracking

The first step in the damage process is the microscopic matrix cracks consisting of the breaking of the resin. They have two forms: transverse or longitudinal. The transverse ones propagate perpendicular to the direction of the mechanical load, whereas the longitudinal ones follow the direction of the loading. Therefore, the two forms depend on the type of applied mechanical stress (tensile, compression, shear or bending, etc.) and the orientation of the fibers within the composite material. With increasing stress, these cracks will progressively propagate and reach the fibers. At this step, the mechanical properties are slightly degraded, and it is difficult to detect these matrix cracks due to the low energy release that they produce. The damage process will either be stopped or will continue with the propagation of the cracks in the less energetic way, which corresponds to the interface between the fiber and the matrix. This will lead to fiber-matrix debonding.

2.2.2. Fiber-Matrix Interfacial Debonding

Fiber-matrix interfacial debonding usually happens when the cohesion of the fiber-matrix is lower than the shear strength of the matrix or when the adherence of the fiber-matrix is weak. The matrix crack induces debonding without fiber breaking. The amount of debonding will increase while the stress increases. This damage mechanism is more energetic than the matrix cracks, but it is still low and does not have a big influence on the mechanical properties. As the matrix cracks and the debonding will propagate, the interlaminar cracks will occur and the load will progressively increase on the fibers, resulting in delamination and the fibers breaking.

2.2.3. Delamination or Interlaminar Cracking

Delamination [41] concerns the laminated composites. It consists of an interlaminar cracking of the resin and leads to the separation between two successive plies. Delamination can be internal or near-surface. It can grow and extend its area, and then it will lead to the failure of the laminated composite. It can be considered one of the most severe damages for laminate composite materials, which explains why many referenced articles focus on detecting it.

2.2.4. Fiber Breaking

Fiber breaking is also one of the main reasons for PMC structure failure; when the stress reaches the fracture strength of the fiber, it will break. It usually happens when the stress direction is similar to the orientation of the fiber. The rupture of a fiber releases high energy and strongly degrades the mechanical properties of the structure. This is why most of the NDT methods are willing to detect such a violent damage mechanism. The final failure of the PMC material is a combination and an accumulation of these various damage mechanisms.

3. Equipment and Setup for Vibration Analysis

A focus on the modes of vibration (how the structure vibrates at specific frequencies) of the structure is given; this is called modal analysis. How to perform it is first introduced to have the basis to understand the linear and nonlinear techniques.

A brief and nice introduction to modal analysis is given in [42]. In a dynamic analysis, like vibration one, we have to introduce the system that excites the structure (the actuator) and all equipment necessary (the input equipment), the system that catches the information (the sensor) and the equipment that processes the output data and displays results (the output equipment), the system that holds the structure, and all additional setup and equipment.

3.1. Fixation Setup

To perform vibration analysis, there exist several ways of fixing the structure according to the boundary conditions we are looking for. The classical one is to suspend the structure, with elastic wires or threads, to obtain free–free boundary conditions. This will isolate the dynamic response of the structure. The other can be the cantilever configuration with the free–clamped condition (one edge clamped) or by putting the structure on absorbing foam. These three configurations can be seen in Figure 6. Some researchers also used the clamped–clamped configuration to perform their analysis. As the vibrations of bridges are often investigated, another method consists of laying the structure on several supports; it can be one support for each edge or even some support in the middle of the structure.

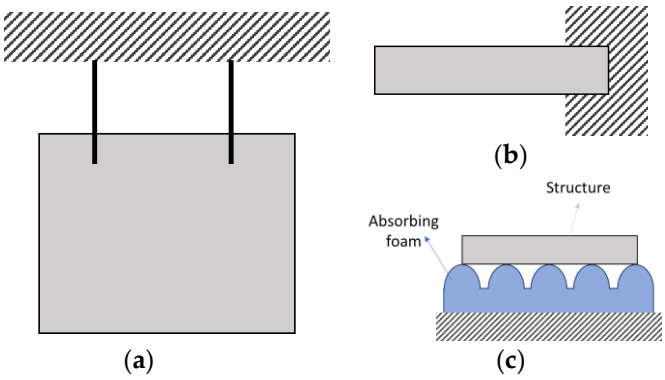

Figure 6. Schematic of different fixation setups: suspended with wire (**a**), clamped in cantilever configuration (**b**), and isolated with foam (**c**).

3.2. Actuators and Sensors

The classical modal analysis is performed with an impact hammer and accelerometers [43]. The hammer has a force sensor to record the input force. For repeatability purposes, it can be replaced by a shaker, which permits applying different kinds of excitation: white noise, sweep signals, etc. It needs a generator and an amplifier to provide an electrical signal. The hammer test is the easiest to perform, it will provide a global view of the vibration of the structure, and it is often used as a first test to obtain the natural frequencies and their damping ratios. Exciting the structure with white noise will give similar results. Once these parameters are obtained, a lot of researchers use different signals, such as harmonic signals, sweep-sine signals, etc., with the intention of focusing on specific modes or working on a large frequency band.

Different actuators and sensors were used in [44,45] to perform modal analyses and identify natural frequencies. The actuators were an impact hammer, a loudspeaker, a fan, and an in situ PVDF piezoelectric transducer (Polyvinylidene fluoride). PVDF and a loudspeaker were used with a white noise generator and piezo-amplifier (the output of the amplifier was 500 V to excite the PVDF), and the accelerometer and the PVDF received the output signal. These articles present a lot of possibilities to perform modal analysis. The

setup necessary to excite with PVDF is given in Figure 7. The SQV 1/500 piezo amplifier is necessary to provide the 500 V at the PVDF.

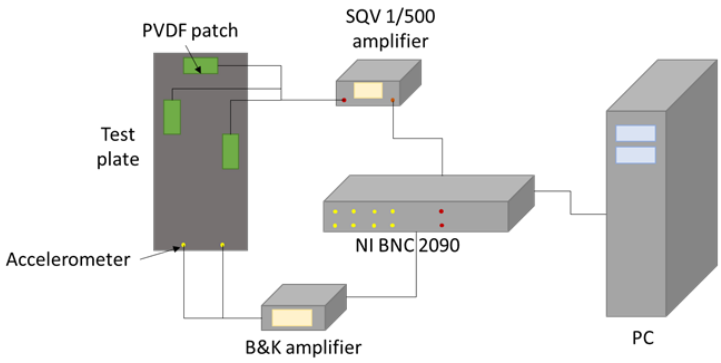

Figure 7. Setup vibration analysis with PVDF as actuator (adapted from [44]).

Piezoelectric transducers deform when they are receiving an electrical signal, which creates vibration, and inversely emit a voltage signal while stress is applied to them (this is known as the piezoelectric effects) [46,47]. There exist several piezoelectric transducers, such as PVDF, PZT—piezoceramic (Lead Zirconate Titanate), MFC (Macro Fiber Composite), and PFC (Piezoelectric Fiber Composite). They have all been used for modal analysis in the literature, where they are mostly surface-bonded, but researchers have investigated the possibility of the in situ transducers [13,48–51]. They can be used as actuators and sensors, but PZT needs a lower amplitude of excitation to excite the structure (20–100 V for PZT against 500 V for PVDF); this is why PZTs are often used as actuators and PVDFs as sensors. Table 3 presents a non-exhaustive list of equipment used for modal analysis.

Table 3. List of possible equipment for modal analysis.

	Equipment	Additional Equipment	Details
Fixation	Foam Wire Clamping system Fixed–fixed	"	"
Input	Impact hammer Manual action Fan	"	"
	Shaker Loudspeaker	Generator—Amplifier	"
	PZT	Generator— Piezo amplifier	40–100 V out of the amplifier
	PVDF		500 V out of the amplifier
	MFC	Generator	"
Output	Accelerometer Laser Vibrometer (LV) Piezoelectric sensors	Analyzer and PC Oscilloscope	"

3.3. Data Processing

The response from the sensors usually goes into an analyzer that directly gives the needed information: Frequency Response Function (FRF) [52], Auto power function [53], Coherence, and Spectrum. There exist several analyzers, such as Simcenter Testlab (also called LMS Testlab from Siemens, Munich, Germany). Without an analyzer, data from the sensors have to be processed to obtain the information that we are looking for. There exist

plenty of data processing techniques; the most famous is the Fast Fourier Transform (FFT) to obtain output in the frequency domain. Some tools, such as, for example, Matlab® software or Python libraries, also allow for extracting such information from the output signal [54]. Some new tools, such as BeagleBoneBlack (from Texas Instruments, Dallas, TX, USA) or Rasberry cards (from Raspberry Pi Foundation, Cambridge, England), propose low and small acquisition systems that permit easily implementing them on operational structures.

3.4. Sensor Placement

In modal analysis, the placement of the sensors is very important to obtain the highest amplitude of the response possible or even to obtain a response. Apart from the LV, the accelerometer and the piezoelectric sensors need optimal placement. There exist several techniques and algorithms to optimize it [55–57]. The easiest way is to make a complete modal analysis of the structure experimentally with an LV or even numerically and to observe the mode shapes in order to see the displacement or the strain field in the structure. Indeed, the accelerometers catch the acceleration of the structure at a single point, which is directly linked to the velocity and then the displacement. On the other hand, piezoelectric transducers catch the stress applied to them, which is directly linked to the strain. Accelerometers and piezoelectric transducers do not give the optimal signal at the same position. An example is given in Figure 8; there is the displacement field of the first four modes of vibration of a free plate, and the accelerometers should not be placed in the blue area in order to record as much acceleration as possible. Obviously, for a free plate, the highest displacement will be on its edge (the red area). In Figure 9, we can see the optimal placement obtained for a set of accelerometers and PVDF transducers using the Effective Independence (EI) method based on the maximum kinetic energy [45].

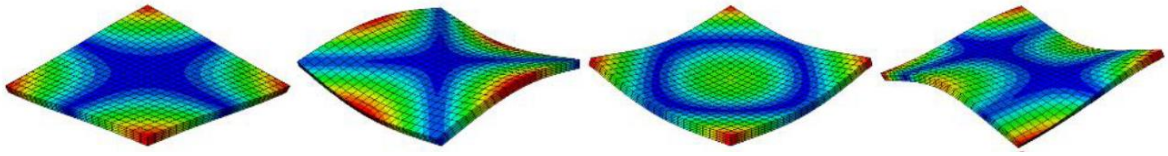

Figure 8. First four modes of vibration of a free–free plate (displacement is shown, blue means no displacement and red maximum displacement).

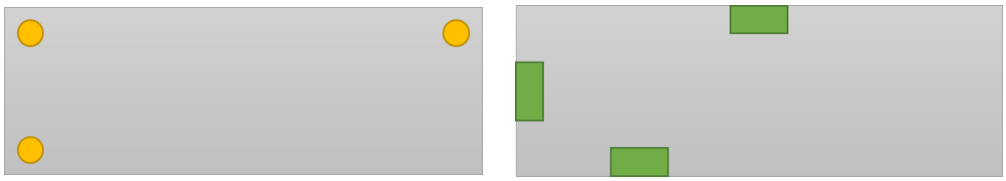

Figure 9. Optimal placement obtained from the Effective Independence (EI) for 3 accelerometers (**left**) and 3 PVDFs (**right**) (adapted from [45]).

4. Vibration Methods for SHM

4.1. Linear Vibration Methods

4.1.1. Natural Frequencies

The natural frequencies of a structure are the frequencies where the structure will tend to vibrate after applying an external force. Using these frequencies to excite the structure will introduce the effect of resonance, which creates a higher amplitude of vibration. They are directly linked to the mass and stiffness of the structure, as well as its boundary condition. This is what pushed many researchers to use them as damage indicators. Indeed, the damage will create a loss of stiffness, which induces a decrease in natural frequencies (Figure 10). Moreover, this technique is one of the cheapest and easiest to perform. In a review published in 1996 [58], it is indicated that the first one to use natural frequency loss as a damage indicator was Lifshitz [59] in 1969.

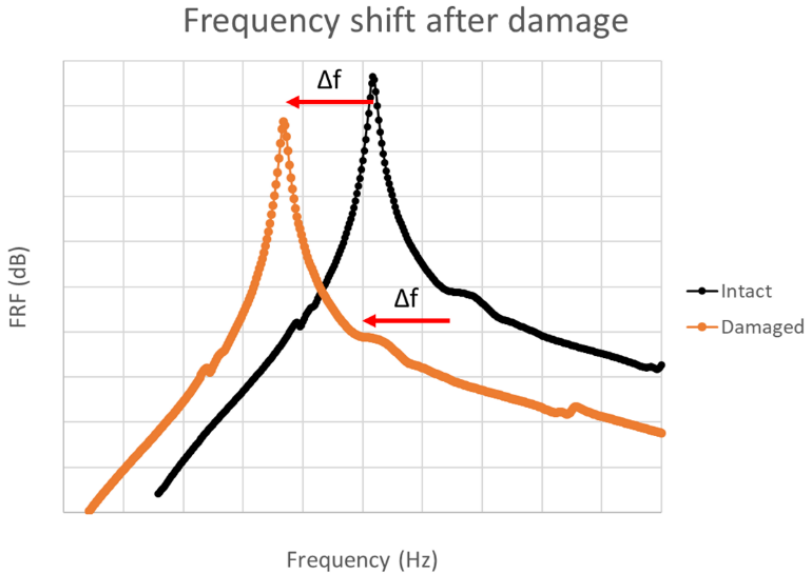

Figure 10. Natural frequency shift induced by damage.

In [60], the change of the first natural frequency in E-glass/epoxy-laminated composite plates with two different dimensions (13 × 6 cm^2 and 19 × 6 cm^2) and three stacking sequences ([90/90/90/90]°, [0/0/0/0]°, and [0/90/0/90]°) with a cantilever configuration (Figure 11) was investigated. Damage was introduced by cutting the inner fibers in two locations: in the middle and at the root of the structure (which plies is unknown). The fiber cutting dimension was 2.1 × 1 cm^2 and 3.1 × 1 cm^2. PZT transducers were used to excite the plate but also to catch the output signal. An oscillating voltage with different amplitudes was transmitted to the actuator (from 40 to 80 V) and the output was displayed on a sensing unit. The frequency was manually varied from 0 to 40 Hz until a sharp increase in the sensing voltage was observed. The frequency of this increase corresponded to the first natural frequency of the structure. The frequency decreased (1.5 to 4 Hz for the smaller plate and 0.3 to 1 Hz for the larger plate) when the structure was damaged for the [90/90/90/90] stacking sequence. However, this was not the case for the other stratifications due to the high stiffness in the [0/90/0/90] sequence.

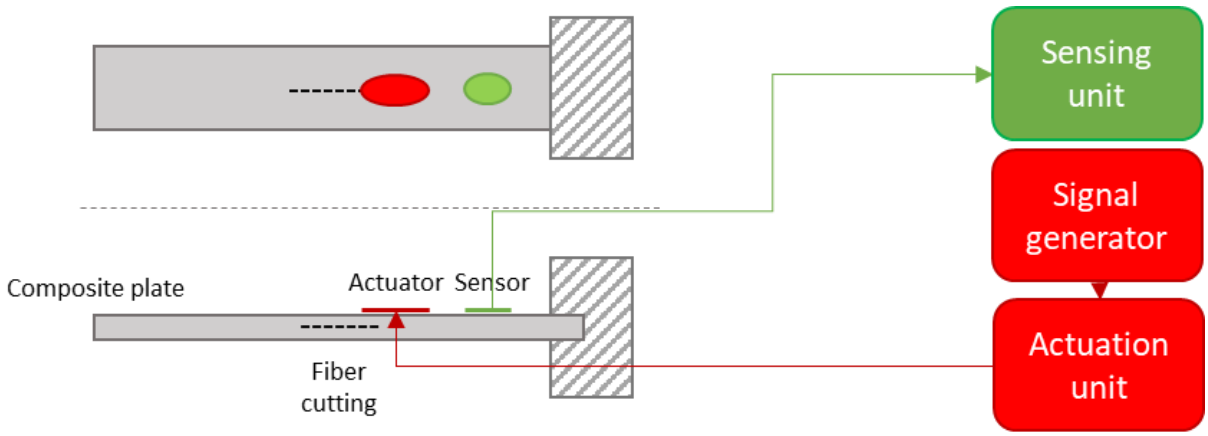

Figure 11. Schematic experimental cantilever setup: middle damage (adapted from [61]).

In [61,62], two kinds of inner piezoelectric transducers, MFC and PFC, were used in glass/epoxy laminate and sandwich beams in a cantilever configuration. Different severities of delamination (10/20/30/40/50/60% of the area of the structure) and crack (2/3/7/14/20/27/34% of the length of the structure) were created in laminates (300 × 32 × 21 mm^3) and only delami-

nation between core and skin (10/30/45/60/75% of the area of the structure) in the sandwich material (300 × 32 × 14 mm^3). The excitation was introduced by displacing the tip of the beam by 0.5 inches, and the transducers caught the vibration of the structure. Here, the change in the first two natural frequencies was investigated. The frequencies decreased when the severity of damage increased; the decrease was almost linear and slow, which meant no clear distinction was possible before a large amount of damage (20% for the delamination, 15% for the crack of the laminates, and 60% for the sandwiches), which meant the small damage could not be detected. The loss of natural frequency was higher in the laminated composite.

In [63], PZTs were surface-bonded and used as actuators and sensors on a graphite/epoxy $[90/+45/-45/0]^\circ$ plate (250 × 50 × 1 mm^3) clamped at one end. The natural frequencies of six modes of vibration were used for several types of damage: a 6.4 mm diameter hole in the center, matrix cracks induced by fatigue testing and mallet hit, and delamination (8%) made of Teflon strip and cut. A signal generator was used to transmit the voltage to the PZT and an LV was used to compare with the results from the PZT. Clear distinctions regarding frequency loss for any type of damage from LV or PZT were not possible.

In [64,65], experimentation was conducted on a plate (305 × 244 × 2.16 mm^3) made of eight plies of carbon/epoxy stack in $[0]_s$. To isolate the dynamical response, the plate was suspended with wires. An impact hammer made the structure vibrate, and the signal from surface-bonded MFCs and accelerometers was caught; then, it was processed in a data acquisition LMS system and displayed on a PC analyzer interface, Testlab. Results were difficult to analyze and no real distinctions between undamaged and damaged structures (made from hole and impact—no information is given regarding the dimensions of damages) were observable. For this reason, the authors used different metrics that compared healthy and damaged signals (see FRF section).

The effects of damage on natural frequencies of the first three modes have been investigated on glass/epoxy laminate (200 × 30 × 8 mm^3) [66] and sandwiches (250 × 40 × 26 mm^3) [67,68] with PVC foam core and glass/epoxy skin on a cantilever configuration. The damages were debonding between the core and skin for the sandwich (from 20 to 180 mm of debonding by 20 mm step) and fatigue induced for the laminate. The structure was excited with a shaker and a power amplifier, and the vibration was sensed with an accelerometer. The excitation signal was a swept-sine around bending mode frequency with an amplitude of 50 mV. The natural frequency decreased with damage severity, and the higher mode seemed more influenced by this severity (Figure 12). In these references, the change in natural frequency was studied and investigated, including, especially, the loss factor and the nonlinear elastic and dissipative parameters. These magnitudes will be introduced later.

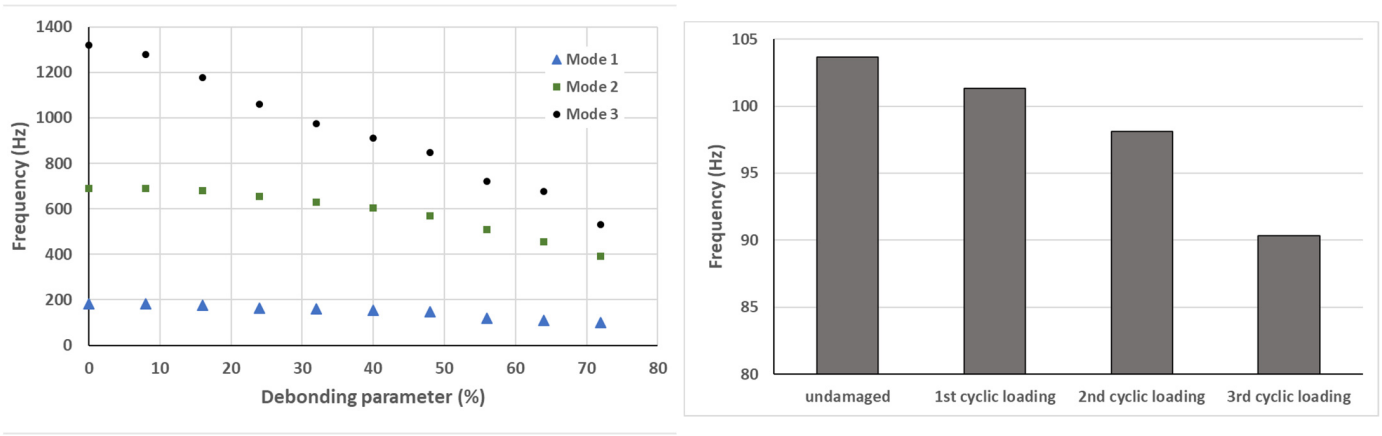

(**a**) (**b**)

Figure 12. Loss of natural frequency with increase in damage severity for sandwiches (**a**) (adapted from [68,69]) and laminate (**b**) (adapted from [66]).

Through these articles, detecting damages from the variation in natural frequencies seems efficient only when damage is already consequent. However, when damage is small (<20%), this technique showed some limits. Table 4 gives additional bibliographical references using this method. Nowadays, it is less and less used because of its high sensitivity to environmental effects, like temperature or boundary conditions.

Table 4. Other articles about the experimental use of natural frequency shift for SHM.

Structure	Fixation	Input	Output	Damage	Description	Ref.
Graphite/epoxy-laminated plate	Fixed in V-blocks		Accelerometers	Delamination (Fluorinated Ethylene Propylene (FEP) patches)	4 first natural frequencies were used to observe that delamination has effects on the frequency loss, and 1/3 of the area of the specimen will lead to 20% of max defect	[69]
Carbon/cyanate-laminated plate	Cantilever configuration	Surface bonded bimorph PZT patch actuator QP25N (150 V) Agilient 33120A waveform generator CX Quickpack Amplifier	LV	Delamination (plastic film)	Natural frequencies are used to identify delamination in composite plates; a small loss in natural frequencies is observed, especially for higher modes (20% decrease)	[70]
Glass/epoxy-laminated beam	Cantilever configuration	Impact hammer G1195 PZT bonded patch (sine sweep signal) Amplifier	PVDF bonded patch Analyzer (HP35665A)	Delamination (Teflon patches)	Natural frequencies shift induced by delamination is used to feed an NN; the natural frequencies became lower when the structure was damaged	[71]
Carbon- and Kevlar/epoxy-laminated beam	Cantilever configuration	Impact hammer PZT	Accelerometer PZT	Delamination (FEP patches)	Natural frequencies decrease is observable for the damaged structure for both PZT and accelerometer sensors	[72]
Circular glass/epoxy-laminated plate	Suspended with 3 flexibles	Loudspeaker Oscillator and amplifier	Accelerometer Oscilloscope	Delamination (impact 45 J)	Natural frequencies tend to decrease when the delamination area gets bigger and bigger; for mode 1 and 6, the natural frequency increases after reaching a delamination area (probably induced by a local change in the geometry)	[73]
Glass/polyester-laminated beam	Suspended by flexible	Impact hammer	Accelerometer Analyzer	Crack	Natural frequencies tended to decrease when the crack size increases, and some modes seemed more influenced by this damage	[74]

4.1.2. Mode Shapes

The mode shapes correspond to the displacement of a structure for a particular natural frequency (a particular mode). The simplest example is the vibration of a fixed string; for each mode, there will be nodes (the fixed part) and antinodes (the maximum displacement) (Figure 13).

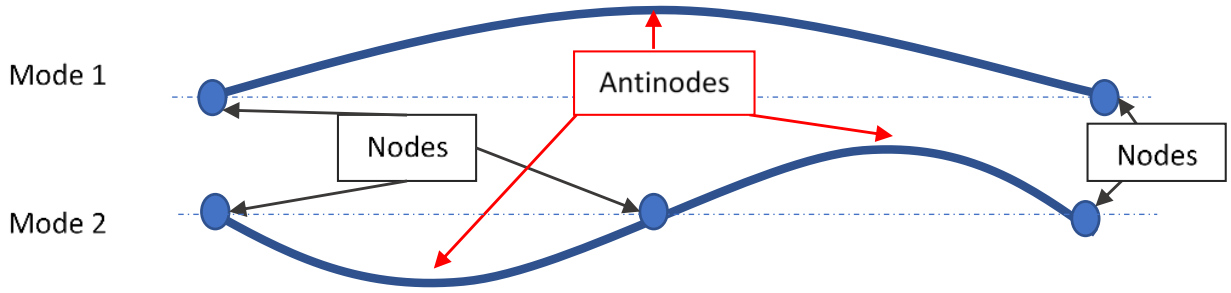

Figure 13. Two first modes of vibration of a fixed string.

The first thing is to obtain the mode shapes of the structure, so it is necessary to perform a modal analysis that takes the vibration measurements at several locations. This means having a network of sensors, moving excitation location and sensor position [42,75], or scanning the structure with an LV.

Several techniques exist using modal shapes to detect and localize damage; the most classical ones are the Mode Shape Displacement difference (MSD) or the use of assurance criteria, such as Modal Assurance Criterion (*MAC*) [76], and criteria derived from it, such as Co-Ordinate *MAC* (COMAC) and others [77]. Damage indexes derived from these criteria can also be used, such as the Mode Shape Damage Index (MSDI).

The *MAC* [78] is the main statistical tool regarding mode shapes. It compares two sets of modal vectors using this formula:

$$MAC(\{\varphi r\},\{\varphi s\}) = \frac{\left|\{\varphi_r\}^T\{\varphi_s\}\right|^2}{\left(\{\varphi_r\}^T\{\varphi_s\}\right)\left(\{\varphi_s\}^T\{\varphi_r\}\right)} \quad (5)$$

where φ_s and φ_r are the modal vectors. *MAC* will be close to one if there exists a linear relationship between two modes (if the vectors have a similar way of moving); otherwise, it will be close to zero (Figure 14). In other words, *MAC* can detect which modes will be affected by the damage. A *MAC* can have similar modal vectors even for an intact structure; this is why the reference of *MAC* from the intact structure is necessary to detect the variation. The *MAC* is also commonly used to see the coherence between experimental and numerical vibration analysis.

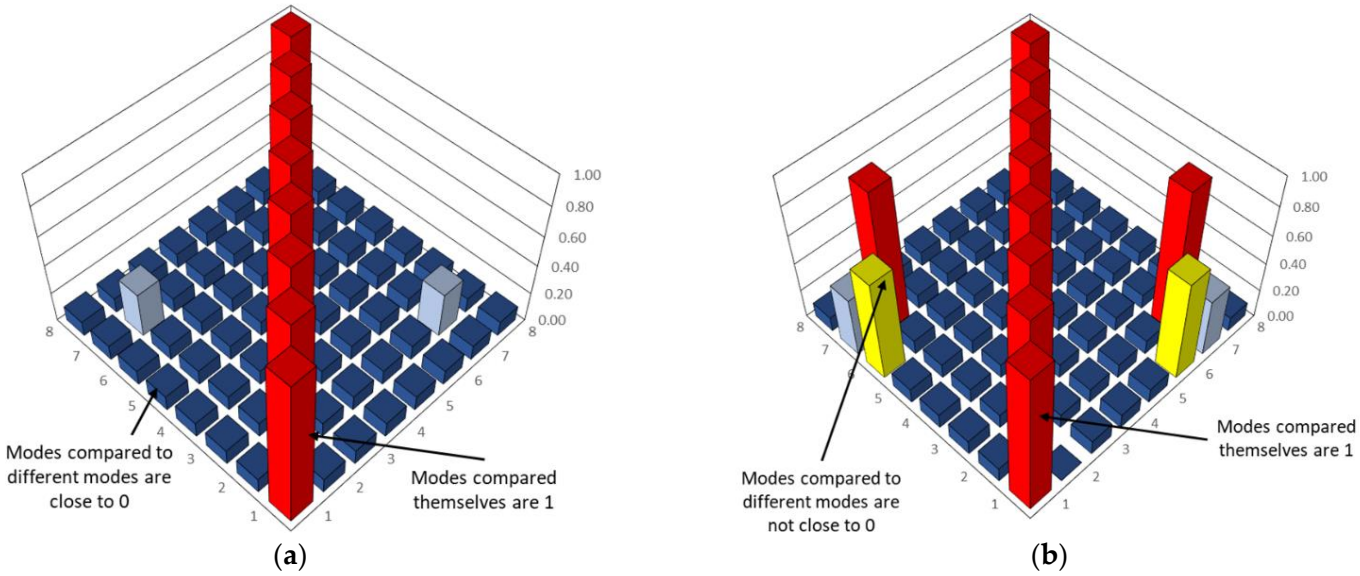

Figure 14. Typical MAC. No similar way of moving of the modes (**a**) and some modes with a similar way of moving (**b**).

In [79], the modal parameters of a hemp fiber/epoxy resin plate (150 × 150 × 5 mm^3) in a free–free condition were used to detect six damage scenarios: cut of a layer with different sizes and positions (20 × 20, 15 × 15, 10 × 10 mm^2 in the center and 20 × 10 mm^2 on the edge), cut of two layers (10 × 10 mm^2), and three layers (10 × 10 mm^2). The classical impact hammer/accelerometer combination was used to perform the modal analysis (Figure 15). A grid of 6 × 6 was created on the plate to acquire 36 data points through the roving hammer method [75]. The MAC and COMAC confusion matrixes between intact plates were created in order to have a reference of both matrixes without damage. Then, it was made between the intact and the six damaged plates, and both detected damage occurrence in the structure. Moreover, the COMAC has higher sensitivity to small damage than MAC.

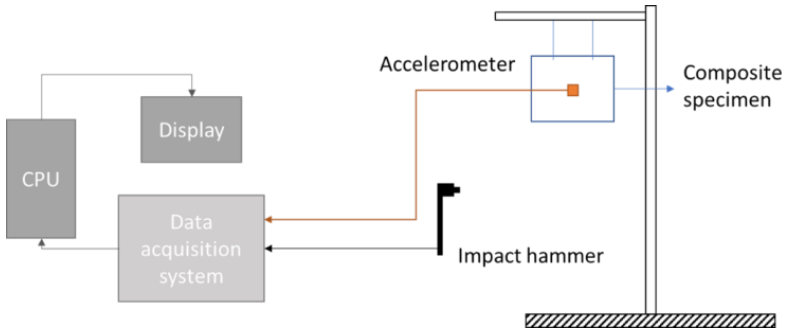

Figure 15. Schematic of the experimental setup (adapted from [79]).

In [80], COMAC was used to detect and localize damage in a helicopter composite blade made of glass-fiber-reinforced plastic with a honeycomb (Figure 16). The structure was suspended to obtain a free–free condition for modal analysis. The actuator was an electrodynamic shaker implemented with a burst random signal, and the sensors were accelerometers positioned on 55 localizations. "Fake" damage was introduced by adding an extra mass of 300 g at one location. The goal of the study was to localize this mass. The modal analysis was performed for both intact and damaged blades. The COMAC detected the presence of damage very close to the exact position.

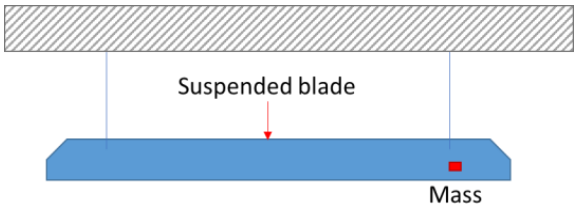

Figure 16. Helicopter blade made of composite suspended with wires (adapted from [80]).

Two derivations of MAC, PrMAC and WECoMAC, were used in [81] on composite plates made of carbon/epoxy. Damage was introduced from a drop-weight impact test, and then compression after the impact test was made in order to determine the compressive residual strength of the structure. The mode shapes were obtained from the roving hammer test at 25 different locations, and damage indicators were calculated at each damage step. PrMAC showed the highest sensitivity regarding damage detection.

To summarize, using changes in mode shape to detect and localize damage has been used by many researchers; however, there exist many techniques and damage indicators, and the classical ones are MAC and COMAC. In [77], a large list of such criteria derived from MAC is given. This technique shows good results in many studies; however, it needs a lot of sensors or heavy measurement processes to acquire the modal deformation accurately. There exist several vibration methods derived from the mode shapes, such as the mode shapes curvature and the modal strain energy, and this is why it is common to see articles using several and comparing them.

Table 5 summarizes other studies that have used the mode shapes methods for the SHM of PMC materials.

Table 5. Other articles about the experimental use of mode shapes for SHM.

Method	Structure	Fixation	Input	Output	Damage	Description	Ref
MSC	T-stiffened panels of carbon/epoxy	Elastic bands	Shaker (sinusoidal wave (0–10 kHz))	LV	Delamination (PTFE Film) Porosity	Change in mode shape displacement between damaged and intact structures was not the best indicator of damage presence	[82]

Table 5. *Cont.*

Method	Structure	Fixation	Input	Output	Damage	Description	Ref
MSC and mode shape slope change	Carbon/epoxy-laminated plate	Suspended with 2 cotton strings	Impulse hammer	Accelerometer	Surface and penetrated crack	The experimental results were not able to detect crack location using both methods (Mode Shape Displacement and Slope Change)	[83,84]
Gapped-Smoothing Method (GSM)	E-glass/epoxy-laminated beam	Cantilever configuration	PZT (Continuous-sweep sine 140 V) Power amplifier	LV (PSV 400 SLV) and PVDF	3 delaminations (Teflon insertion), impact damage, and saw-cut	GSM is able to localize damage through LV or a network of PVDF	[85]

4.1.3. Mode Shape Curvature

The mode shape curvature is the second derivative of the mode shapes. It can be calculated from the central difference method as [86,87]:

$$\varphi''_{ij} = \frac{\varphi_{i+1} - 2\varphi_{ij} + \varphi_{i-1}}{h^2} \tag{6}$$

where φ_{ij} is the jth mode shape of the measurement point i and h is the distance between points $i + 1$ and $i - 1$.

The first step is usually to determine the difference in mode shape curvatures (named Mode Shape Curvature criterion (*MSC*)) between intact and damaged structures:

$$MSC = \Delta\varphi'' = \left|\varphi''_d - \varphi''_i\right| \tag{7}$$

The largest value will give the location of the damage (Figure 17). As for the mode shapes method, the main disadvantage is the number of sensors needed to obtain the most accurate results.

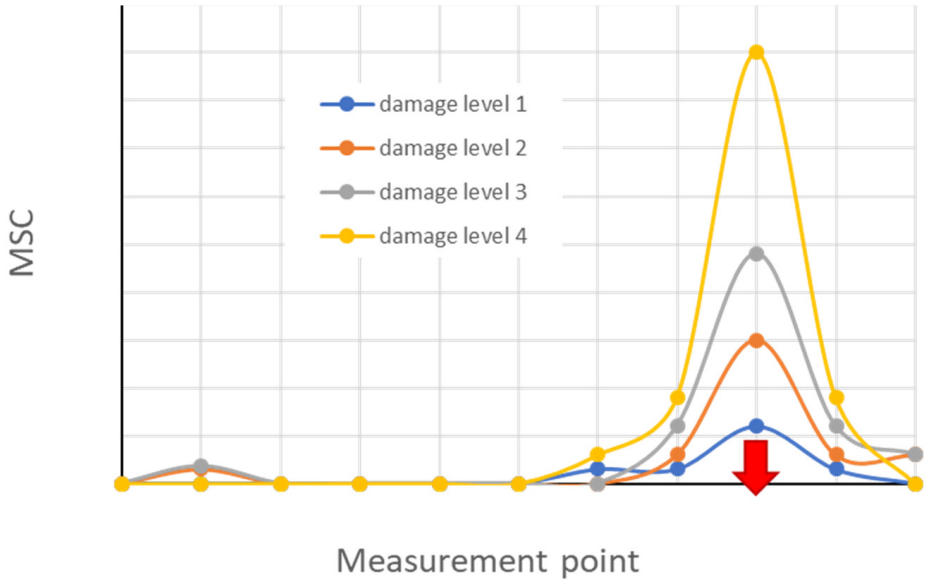

Figure 17. Example of MSC for a different level of damage—damage at the red arrow.

Damage indicators have been derived from the *MSC*. The classical step is to normalize the *MSC* (*NMSC*) and then the Normalized Curvature Damage Factor (*NCDF*) [88]:

$$NMSC = \left[1 + \frac{\Delta\varphi''}{max(\Delta\varphi'') - min(\Delta\varphi'')}\right]^2 \tag{8}$$

$$NCDF_i = \sum_{j=1}^{n} NMSC \tag{9}$$

There exist a lot of possible damage indexes, such as Modal Curvature Change Rate (MCI) and Curvature Mode Difference (CMD).

Modal curvatures were used in [89] in order to detect damage in glass/epoxy plates in a cantilever configuration. The modal analysis was performed with 10 × 5 localization for the PCB impact hammer, and a PCB accelerometer was fixed on the end of the plate. The damage was a crack made from a 1 mm thick blade positioned at 10% of the length of the structure close to the fixed end. NCDF detected well the damage position.

In [90,91], the modal shape curvature was tested on a carbon/epoxy beam (241.3 × 25.4 × 1.76 mm^3) in a cantilever configuration damaged from different sources: an impact, a saw-cut notch, and three different types of delamination (Figure 18). The modal analysis was performed using the PZT or impact hammer as actuators and 16 PVDF as sensors, all surface-bonded (Figure 19). Both NCDF and the DI were used to localize damage; these methods were efficient for three damage scenarios—the saw cut, the impact, and the delamination far from the fixed end—but the conclusion that more sensors are necessary for the two other damage scenarios was made (the two delaminations close to the fixed end).

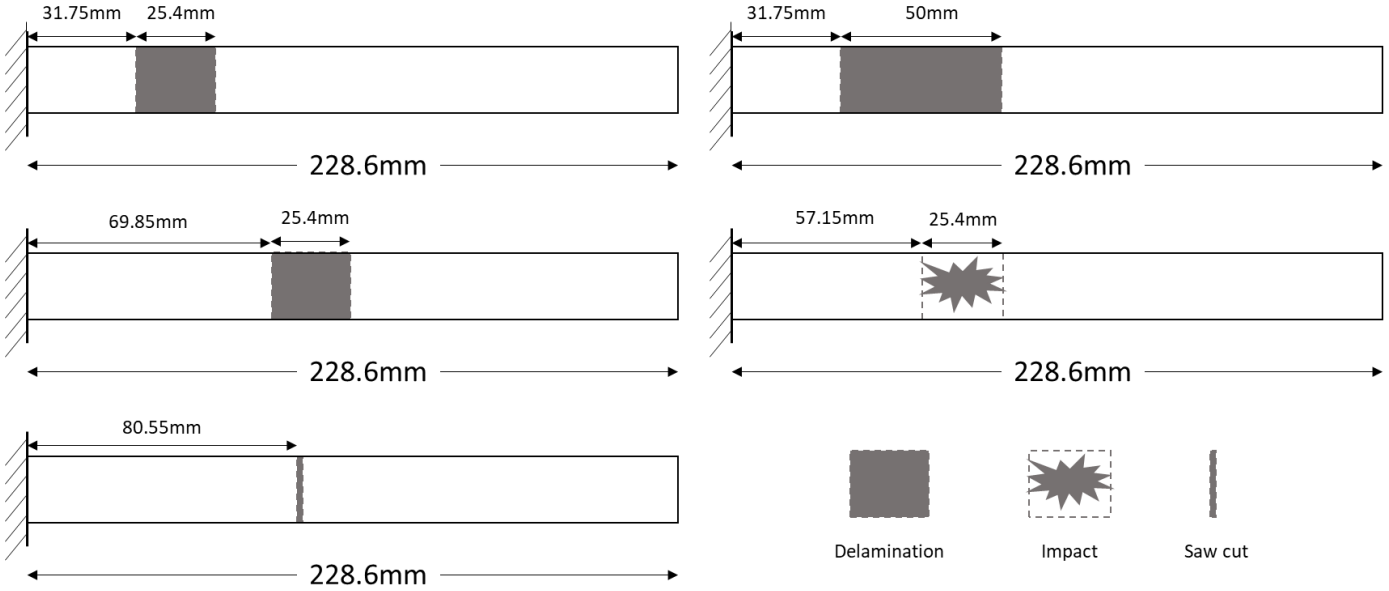

Figure 18. Different damage made on carbon/epoxy cantilever beam (adapted from [90,91]).

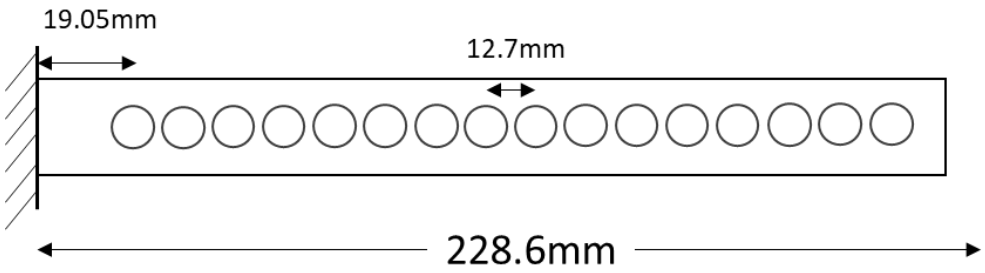

Figure 19. Schematic of the 16 PVDF sensor layout (adapted from [90,91]).

Table 6 summarizes other studies that have used the mode shapes curvatures methods for the SHM of PMC materials.

Table 6. Other articles about the experimental use of mode shapes curvature for SHM.

Method	Structure	Fixation	Input	Output	Damage	Description	Ref.
MSC	T-stiffened panels of carbon/epoxy	Elastic bands	Shaker (sinusoidal wave (0–10 kHz))	LV	Delamination (PTFE Film) Porosity	MSC showed that it can detect delamination accurately, but porosity was not detectable	[82]
MCI and CMD	Carbon/epoxy-laminated beam	Cantilever configuration	Modal hammer	Accelerometer	Delamination (Teflon patch)	CMD showed higher sensitivity than MCI to localized damage	[92]
MSC	Carbon/epoxy beams	Suspended on a frame	Shaker (periodic chirp) Impulse hammer	LV	Delamination and crack	The damage was identified efficiently by the MSC	[93]

4.1.4. Modal Strain Energy

Modal Strain Energy (MSE) is the energy that is stored in the structure for each mode of vibration. According to [94,95], the MSE methods are more sensitive to SHM than the natural frequencies and mode shapes. Many articles use this method on offshore platform structures.

In [96], the ways of calculating MSE for a beam and a plate were given. A review of MSE-based methods for SHM was made in [97]. Four groups were introduced: Damage Indexes (DI), such as Stubbs' DI (SDI) or MSE Decomposition (MSED), Modal Strain Energy Chance (MSEC), Cross-Modal Strain energy (CMSE), and others. In that review, the methods, their calculations, and an experimental study using them were presented. Moreover, a lot of other methods derived from MSE can be found in the literature.

Several articles [84,98,99] used the MSE method on several composite structures; for example, in [98], on a carbon/epoxy plain-woven laminate ($310 \times 222 \times 2.2$ mm^3), the damage was a surface crack (16×1 mm^2) made from a knife located in the middle of the small dotted area in Figure 20. First, a tensile test was performed to determine the mechanical properties of the material. The modal analysis was performed with an impact hammer and an accelerometer fixed on the plate (Figure 20). The total (U_k) and sub-region (delimited by the grid—$U_{k,ij}$) strain energies induced by mode shapes for healthy and damaged plates were calculated from plate formulation. From these equations, the fractional energies ($F_{k,ij}$) for healthy and damaged (*) plates, and the damage index (β_{ij}) and its normalization (Z_{ij}) for each sub-region, were calculated as follows:

$$F_{k,ij} = \frac{U_{k,ij}}{U_k} \tag{10}$$

$$\beta_{ij} = \frac{\sum_{k=1}^{m} F^*_{k,ij}}{\sum_{k=1}^{m} F_{k,ij}}; \qquad Z_{ij} = \frac{\beta_{ij} - \overline{\beta_{ij}}}{\sigma_{ij}} \tag{11}$$

where $\overline{\beta_{ij}}$ and σ_{ij} are the mean and standard deviation. This damage index was able to localize it accurately after using at least three modes of vibration by creating a map of DI on the (x,y) position.

The same helicopter blade [80,100] as used with the COMAC method previously discussed (Figure 16) has been used, and the "fake" damage was a mass adding. The modal analysis was performed with an impact hammer and shaker with a burst random signal; the sensors were 55 accelerometers. The method used to calculate strain energy was based on a Euler–Bernoulli beam and used the modal shape curvature. These calculations are similar to the previous one of the plates. The main goal is to calculate a damage index. The modal strain energy methods showed higher sensitivity than COMAC and were able to detect and localize damage, with a high value on an XY map.

Table 7 summarizes other studies that have used the modal strain energy methods for the SHM of PMC materials.

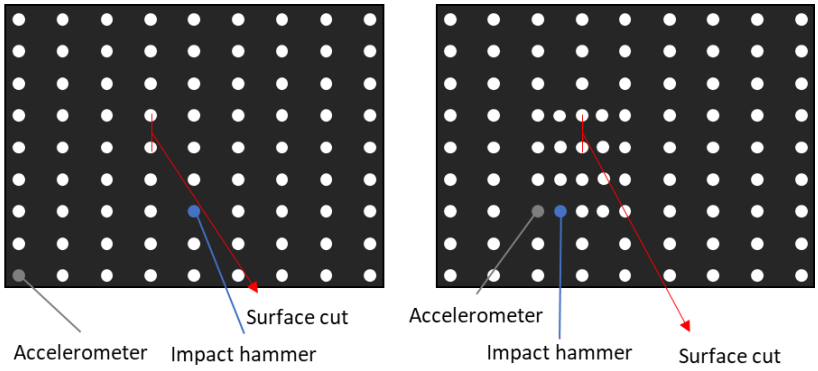

Figure 20. Woven laminate and the grid of measured points for global and local testing (adapted from [98]).

Table 7. Other articles about the experimental use of modal strain energy for SHM.

Method	Structure	Fixation	Input	Output	Damage	Description	Ref.
MSEC	Carbon/epoxy-laminated plate	Suspended with 2 cotton strings	Impulse hammer	Accelerometer	Surface and penetrated crack	MSEC was able to locate both types of damage	[83]
MSE and Differential Quadrature (DQM)	Carbon/epoxy-laminated plate	Suspended with 2 cotton strings	Impulse hammer	Accelerometer	Surface and penetrated crack	For MSE, peaks were present around the location of damage, but some also occurred at other positions; this is why the DQM was implemented, and very good results were obtained with it	[84]
MSEC	E-glass/epoxy-laminated beam	Cantilever configuration	PZT (sweep sine 140 V) Power amplifier	LV (PSV 400 SLV) and PVDF	3 delaminations (Teflon insertion), impact damage, and saw-cut	Strain energy detected well the location of damage, except for special cases with some doubt caused by other high value	[85]
MSECR	E-glass/epoxy skin and PVC foam for sandwich beams	Cantilever configuration	Electrodynamic shaker	Accelerometer	Debonding + remove face (Teflon sheet)	MSECR correctly located damage for single and multiple damage cases	[101]

4.1.5. Modal Flexibility

The modal flexibility method (MFM or MF) is another kind of damage detection technique that seems more sensitive than others and needs less experimental data. The modal flexibility is defined as a matrix:

$$[F] = \sum_{i=1}^{n} \frac{1}{f_i^2} \{X\}_i \{X\}_i^T \tag{12}$$

where f_i is the i-th natural frequency and $\{X\}_i$ is the mass normalized mode shape vectors. What is interesting to observe using MFM is the flexibility difference between undamaged and damaged structures:

$$[\Delta F] = |[F_D] - [F_U]| \tag{13}$$

The highest value of variation will give the location of the damage (Figure 21).

In [102], the MF was also compared to other methods previously seen (Figure 22). In this experiment, the MF seemed the most accurate SHM method.

In [103], the MF and a derivate damage indicator (MDI) were used on a carbon fiber bi-directional corrugated sandwich panel with the dimensions 200 × 200 × 15 mm^3. A grid of 9 × 9 points was created on the surface in order to obtain the vibration at different locations and localize the damages. They created two debonding (1.2% of total area) and three core damage (0.3% of total volume of the core) cases, with single and multiple damage cases. The vibration analysis was performed by suspending the plate, and with

two accelerometers and an impact hammer, an LMS signal analyzer stored all of the output and input data of the first four modes of vibration. Only the MF was not able to clearly distinguish the damage location, as several peaks with similar amplitude were observable. These peaks also occurred in the MDI, but the peak close to the damaged area had a higher value, which avoids the fake damage detection of the MF. They concluded that the new MDI is efficient in detecting single and multiple damages in composite structures.

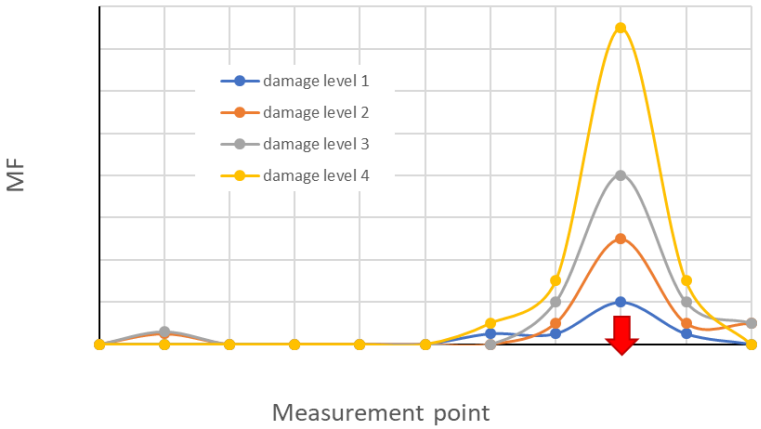

Figure 21. Example of flexibility change for different levels of damage—damage at red arrow.

Case	COMAC	ECOMAC	MSC	MSE	MF
1	X	O	O	O	O
2	X	X	OO	O	O
3	X	X	OO	OO	OO
4	X	OO	OO	O	O
5	X	X	X	X	O
6	X	OO	O	O	O
7	X	OO	X	OO	OO
8	X	OO	OO	OO	O

O: damage detected; **X**: damage not detected; **OO**: damage detected not accurately

Figure 22. Comparison of MF with mode shapes, curvature, and strain energy methods for locating the different damage scenarios (adapted from [102]).

4.1.6. Damping

Damping corresponds to the energy of dissipation of material (as seen in Section 2.1). In [104], a review of the use of damping for SHM is provided. According to this article, the change in damping has higher sensitivity than natural frequencies or mode shapes to detect damage, but research is still in progress. The simplest analysis of damping is the difference in damping between intact and damaged structures; usually, it will be higher when the structure is damaged, and it shows higher sensibility than the change in natural frequency (Figure 23). Damage identification using damping can either be linear or nonlinear.

In modal analysis, the damping ratio is mostly calculated from the −3 dB method (or half-power bandwidth) (Figure 24) in the frequency domain, but time domain and time–frequency domain methods are also found in the literature. In the time domain, the most frequent method used is the logarithmic decrement [105], and in the time–frequency domain, the use of analyzing wavelets, such as the Gabor wavelet, is necessary [106]. There exist several quantities to define damping:

$$\eta = \frac{1}{Q} = 2\zeta = \frac{\%Cr}{50} = \tan\Phi = \frac{\Delta\omega_{3dB}}{\omega_0} \tag{14}$$

where η is the loss factor, Q is the damping of the quality factor, ζ is the damping ratio, %Cr is the percent of critical damping ($\%Cr = 100\% \times \zeta$), and Φ is the phase angle between cyclic stress and strain.

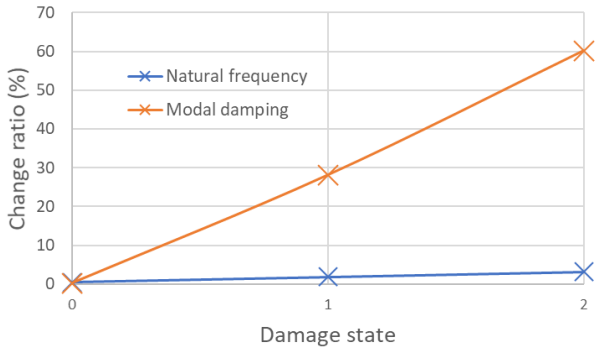

Figure 23. Difference of sensibility between damping and natural frequency methods (adapted from [104]).

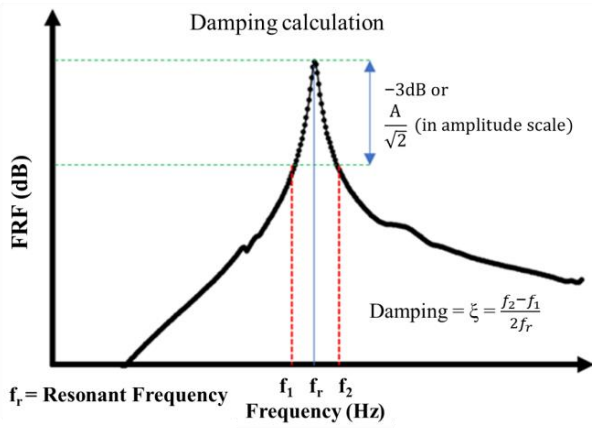

Figure 24. −3 dB method.

Damping to detect damage is also used with a Damage Index, and it is often mixed with other methods, such as modal shape, natural frequencies, modal strain energy, etc.

In [65], in addition to comparing natural frequency, a comparison of the difference in damping between damaged and intact carbon/epoxy plates was made in a free–free configuration from impact hammer excitation and two accelerometer sensors. Two damages were studied: one impact damage and one hole (of unknown diameter) both in the center of the plate. No specific pattern in the difference in damping ratio was detectable.

In [66–68], the effects of damage on loss factors were also investigated; on the laminated and sandwich composite with delamination and fiber cutting, it was shown that the loss factor increased with damage severity (Figure 25).

In [107,108], a method was developed using damping mixed with Plane Shape Function (*PSF*) to localize damage. The name is Damping Damage Indicator (*DaDI*). It was tested on a woven carbon/phenolic plate damaged from impacts and quasi-static pressure. The structure was suspended with two nylon strings to obtain a free–free configuration. The *DaDI* needs modal strain shapes and modal damping factors to localize damage. The excitation was made with an electromagnetic shaker and a multisite excitation force, and the sensor was LV at four different points. The *PSF* for mode n and *DaDI* at coordinate (*i*,*j*) was calculated as:

$$PSF_{ij}^{n} = \frac{\left|x\varepsilon_{ij}^{n}\right|}{max\left|x\varepsilon_{ij}^{n}\right|} + \frac{\left|y\varepsilon_{ij}^{n}\right|}{max\left|y\varepsilon_{ij}^{n}\right|} \qquad DaDI_{ij} = \frac{\sum_{n=1}^{N}\left(PSF_{ij}^{n}\ \Delta\eta_{n}^{D}\right)}{\sum_{n=1}^{N}\left(PSF_{ij}^{n}\right)} \tag{15}$$

where $x\varepsilon_{ij}^{n}$ and $y\varepsilon_{ij}^{n}$ are the strain in both directions and $\Delta\eta_{n}^{D}$ is the difference in damping ratio between damaged and intact structures. In the article, *DaDI* seems to determine the location of both damages well. Adding mass to the structure with transducers may decrease the accuracy of this method. In [109], similar experiments were conducted on carbon/epoxy plates. Several indexes were used, such as Multiparameter Damage Indicator (MuDI), which is created from two others, the *DaDI* and the frequency damage indicator (FreDI), to localize the damage. A weighting function was introduced to emphasize the role of FreDI or *DaDI* in the computation of MuDI; this weighting function showed the importance of the correct localization of damage.

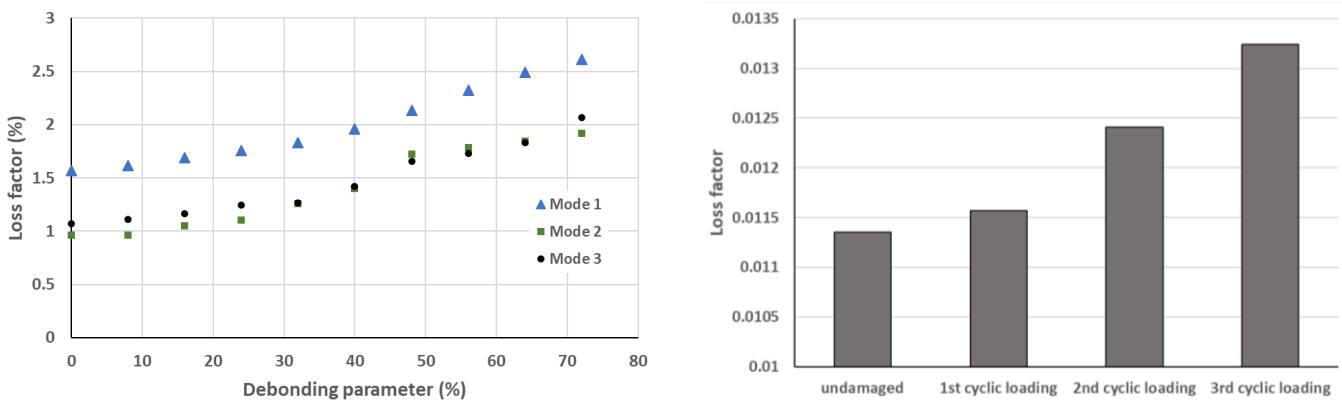

(**a**) (**b**)

Figure 25. Loss factor increase with the increase in damage severity for the sandwich (**a**) (adapted from [68,69]) and laminate (**b**) (adapted from [66]).

4.1.7. Frequency Response Function Metrics

Comparing the FRF of intact and damaged structures can be a way to detect damage [110]. Several damage indicators based on FRF have been introduced in the literature [64], such as the Frequency Domain Assurance Criterion (FDAC) [111] or the Frequency Response Assurance Criterion (FRAC) [112].

In [64,65,113], the metrics introduced were tested on a carbon/epoxy plate suspended in a free–free configuration; the sensors were accelerometers and MFC, and the actuator was an impact hammer. The plates were damaged by a central hole and an impact (dimensions are unknown). The change in natural frequencies was not sufficient to detect damage, but the metrics gave interesting results, and it seemed that metrics using more than one sensor gave higher sensitivity.

4.1.8. Transmittance or Transmissibility Function (TF)

TF is a technique to determine the localization of the damage. It is built from the ratio of the vibration response of the structure at two separate locations and the location of the input force. It is often written as T_{ij}^{k}.

$$T_{ij}^{k} = \frac{x_{i}^{k}(\omega)}{x_{j}^{k}(\omega)} \tag{16}$$

where x is the displacement at i and j location, where the force is applied on k. TF can also be calculated from the velocity of the structure instead of displacement. Then, detecting damage is performed with a damage indicator on a frequency range $[\omega_1; \omega_2]$, which compares the TF for healthy (h) and damaged (d) structures.

$$D_{ij}(\omega_1;\omega_2) = \frac{\int_{\omega_1}^{\omega_2} \left| T_{ij}^{h}(\omega) - T_{ij}^{d}(\omega) \right| d\omega}{\int_{\omega_1}^{\omega_2} \left| T_{ij}^{h}(\omega) \right| d\omega} \tag{17}$$

A review of TF is given in [114]. This technique is mostly used numerically, but with a network of sensors or an LV, it can be used experimentally. One issue with this method is the selection of the frequency range to obtain accurate results. As we can see in Figure 26, damage on paths 2–3 can be detected with the frequency range [0, 39] but not with the range [0, 300]. Usually, the upper value of the range is chosen as the first natural frequency of the structure. The position of the input force will also have a strong influence on the result.

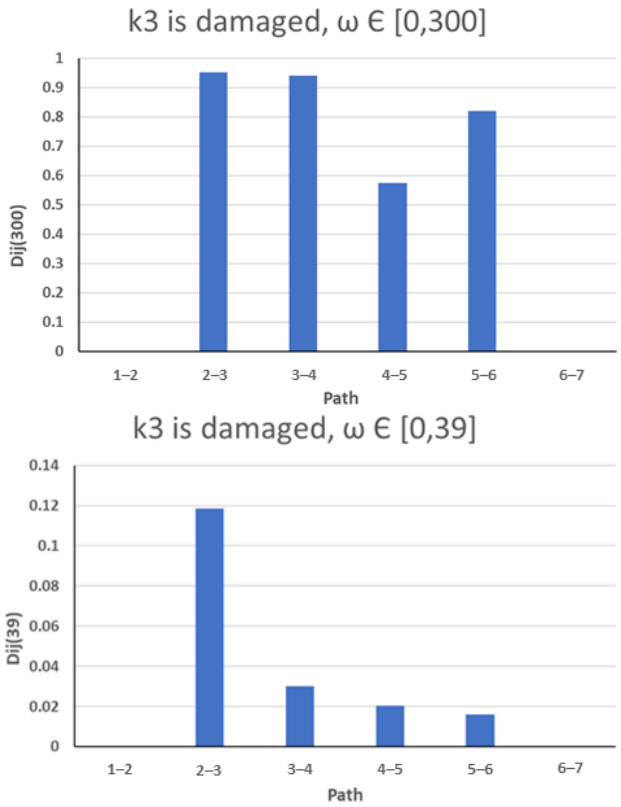

Figure 26. Damage indicator of TF for different frequency ranges, damage on path 2–3 (adapted from [114]).

To summarize, in the review, they said that the perfect localization of the damage is possible when the damage is located next to the input force localization or by choosing the correct frequency band, which means the global vibration of the structure has to be known.

In [115], TF was used on a cantilever fiberglass beam ($112 \times 1.18 \times 0.635$ cm^3) with a PZT actuator and accelerometers or PZT patches as sensors (Figure 27). The PZT actuator was excited with a random noise signal coming out of an amplifier. It was shown that using an impact hammer and shaker as actuators did not give nice repeatability of the experimentation, but the PZT actuator gave correct repeatability. Translational and curvature TF were investigated. The damage was created by bonding a steel plate ($5.08 \times 5.08 \times 0.635$ cm^3) to the beam between paths 1 and 2. The translational and curvature TF showed efficiency in localizing moderate damage. The curvature one seemed more accurate while the frequency range was higher (10–20 kHz). A very high-frequency range did not allow for detecting damage, and the curvature TF seemed more sensitive for small damage.

In [116], the modal analysis of a wind turbine blade made of fiberglass in a free–free boundary condition was performed. PZT patches were used with a periodic chirp signal at 200 V as an actuator and an LV as the sensor. The damage was introduced as "fake" damage by clamping a steel plate ($203.2 \times 152.4 \times 19.05$ mm^3) near one edge close to the path 11–15. The damage indicator of the TF indicated the correct location for the "fake" damage (Figure 28); this damage indicator should be near 0 for the healthy structure and healthy paths.

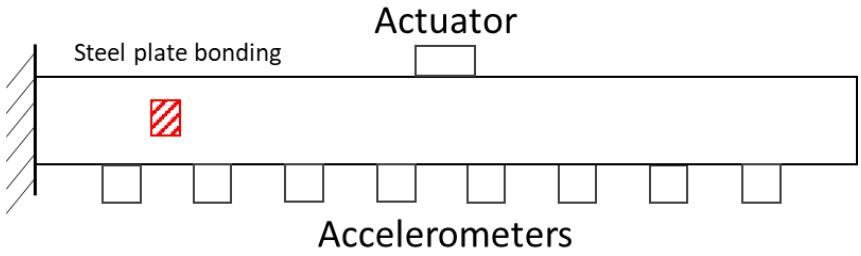

Figure 27. Experimental setup of the cantilever fiberglass beam with 8 accelerometers and one PZT actuator (adapted from [115]).

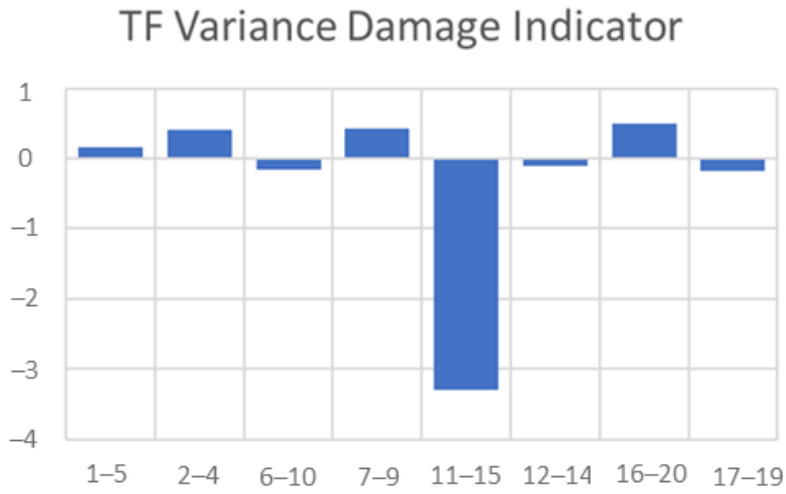

Figure 28. TF variance DI, damage between path 11–15 (adapted from [116]).

In [117], two models based on transmittance function were created and studied, the first one using only one transmittance model for the healthy state named "single transmittance model" (STM) and the second one using several transmittances models, the "multiple transmittance models" (MTM). Both models were based on a data-based response-only methodology using the autoregressive with exogenous excitation model (ARX). The study was conducted using 29 composite beams made of carbon fiber in unidirectional or woven fabrics. The damage was introduced in the middle of two beams with an impact hammer at 5 and 15 J. The modal analysis was performed in a cantilever configuration with a shaker as an actuator and two accelerometers. The STM scheme detected most of the damage, but it gave some false alarms and failed to detect some damage; on the other hand, the MTM scheme was able to detect all damage cases without false alarms.

4.1.9. Wavelet Transforms

In vibration analysis, the Wavelet Transform (WT) has been used a lot to process the vibration data coming from various sensors. The principle relies on dividing a time-series signal into a set of sub-signals (wavelets) and extracting data from these sub-signals. There exist different kinds of Wavelets, such as Daubechies and Symlet. A review of WT is given in [118].

In [119], small delamination (0.11%, 0.167% and 0.22% of the total surface) of glass/epoxy plates ($360 \times 250 \times 4$ mm^3) with piezoelectric transducers (one actuator and four sensors) was studied. The signals were decomposed for each sensor into 16 sub-signals with Daubechies Wavelet, and a damage indicator was introduced for intact and damaged structures based on the energy of these sub-signals and then by setting a threshold for this damage indicator. The conclusion was that using a threshold of 20% with WT helps to detect small delamination of an area superior to 0.12% of the total area of the structure. In Table 8, it is possible to see the damage indicator calculated for each sub-wavelet. If one of the sixteen sub-wavelet damage

indicators are higher than the threshold, the authors considered the delamination detected (grey cells).

Table 8. DI results for 3 different delamination areas and 16 sub-wavelets with a threshold at 20% [120].

		Delamination Area of the Total Area		
		0.11%	**0.167%**	**0.22%**
Sub-Wavelets	0	1.703	2.491	0.908
	1	8.053	6.078	21.32
	2	0.403	3.718	−1.005
	3	−0.634	2.197	−1.818
	4	−14.10	−45.38	−6.603
	5	12.83	5.221	36.42
	6	0.395	1.546	3.626
	7	6.811	5.449	17.76
	8	0.961	3.068	−2.736
	9	3.575	−0.045	8.691
	10	0.561	4.663	−1.279
	11	0.165	1.226	−2.389
	12	−12.30	−31.87	−8.129
	13	3.143	−2.751	17.04
	14	0.412	4.026	−1.193
	15	0.602	3.390	0.225

4.2. Nonlinear Vibration Methods

As the damage mechanisms in a composite structure are complexes, the tendency nowadays is to focus on nonlinear vibration methods, as they give the opportunity to increase accuracy and detect smaller damages. Most of these methods consider that the damage of the composite structure will induce nonlinearity, caused by some microcracks, delaminations between layers, or fiber breakages. As an indication, opening and closing consecutive phases of a matrix cracking can generate a nonlinear response.

This behavior has been investigated in many studies, and some nonlinear methods have emerged. Some of them cross the boundary between ultrasonic and vibration fields, but they are still introduced to see the possibilities and the potential setup needed. Moreover, as these methods are less used than linear ones, the number of experimental studies focused on PMC materials is smaller.

4.2.1. Single Frequency Excitation (SFE) and Sub-/Super-Harmonics Generation

By definition, a harmonic is a multiple of a fundamental frequency (which is the harmonic n°1). Sub- and super-harmonics are ratios of this harmonic, the sub-harmonics are $\frac{f}{n}$, and super-harmonics are $n \times f$ (with f the harmonic). The damage detection technique relies on the fact that by exciting the structure through a harmonic signal, the response will only show this harmonic for an intact structure, and will show super-harmonics (or higher harmonics) and sub-harmonics of smaller amplitude for a damaged structure (Figure 29).

Some authors highlighted the fact that better results can be obtained using a frequency of excitation corresponding to a ratio of a natural frequency, ½, 2, etc. Higher amplitude of sub- and super-harmonic can be observed. But a lot of them used ultrasonic frequency.

The nonlinearities can also be observed as distortions in the time-domain response (Figure 30). It can be velocity, acceleration, or voltage signal distortions. A phase portrait of velocity vs. displacement or acceleration vs. velocity graphs can be made. The phase

portrait should not show any distortions for an intact structure (circle or ellipse), while it should show some for a damaged structure (Figure 31).

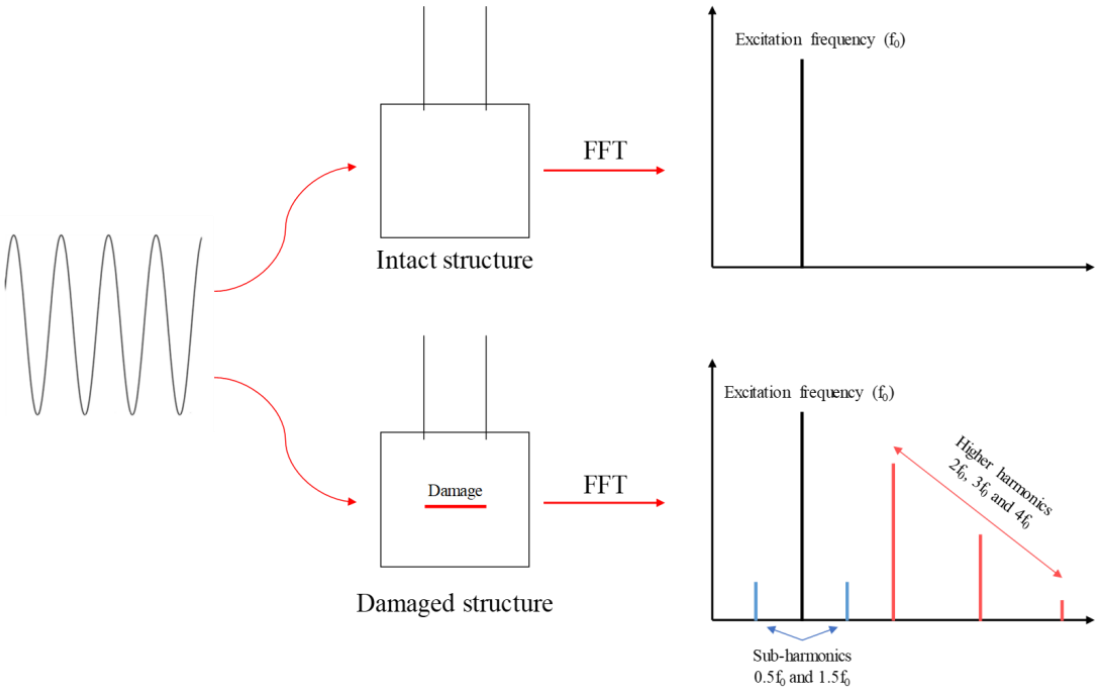

Figure 29. Schematic of the SFE method (adapted from [120]).

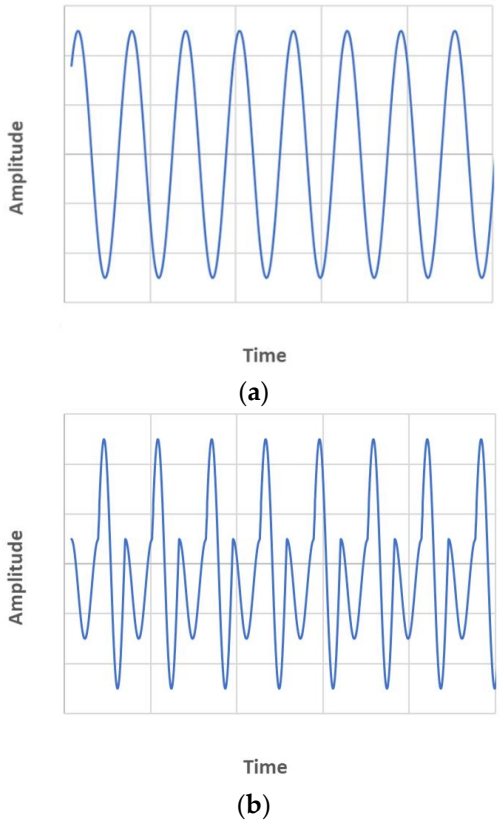

Figure 30. Time-domain signal of the voltage of the structure under a harmonic signal excitation—intact (**a**) and damaged (**b**) structures.

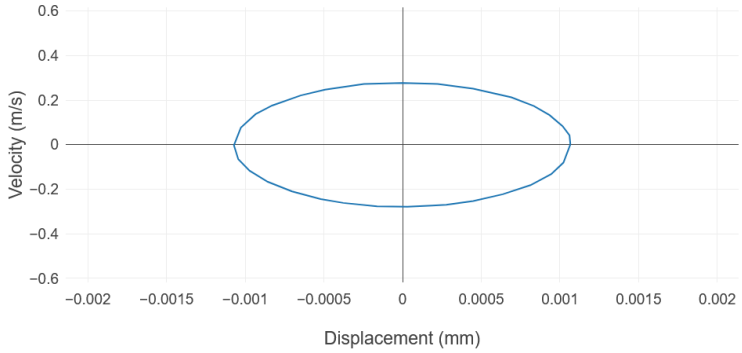

(**a**)

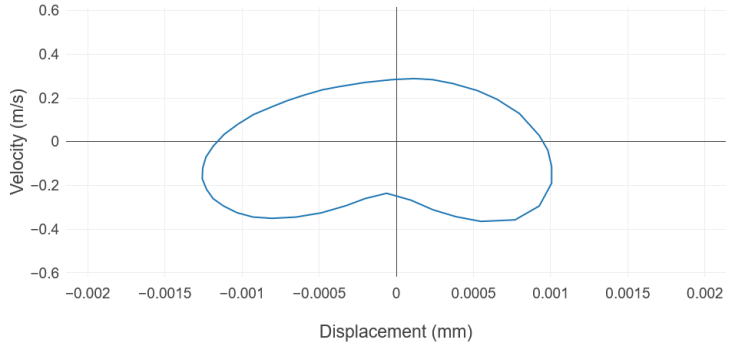

(**b**)

Figure 31. Phase portrait: velocity vs. displacement for intact (**a**) and damaged (**b**) structures (adapted from [121]).

In [120], three different methods to detect damages in carbon/epoxy laminate plates ($200 \times 200 \times 2.08$ mm^3) were investigated. The structure was suspended freely with thin wires and the damages were introduced by inserting Teflon sheets located under the fourth plies from the surface (Figure 32), which created delamination (35×35, 40×40 and 45×45 mm^2). One of these methods was the SFE, and five piezoelectric transducers were used, one as an actuator and four as sensors. They were bonded onto the surface. From the actuator, the plate was excited with a sinusoidal wave of 120 V and with a frequency varying from 20 to 100 kHz. The additional equipment was a generator, a power amplifier, and an oscilloscope. Higher harmonics in the damage cases were observable. Some frequencies (20–40 kHz) have higher sensitivity, which means the choice of the best one is important. A damage indicator based on the amplitude of harmonics was defined to easily detect damage.

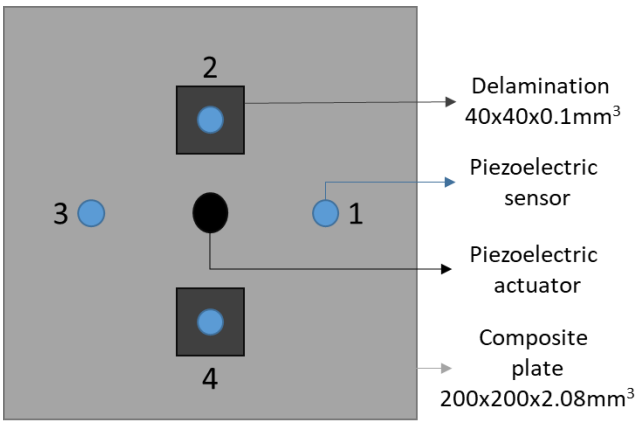

Figure 32. Composite plate with 5 PZT transducers and 2 delaminations (adapted from [120]).

In [122], the SFE methods were tested on a PMC plate embedded with an in situ PVDF sensor and a shaker actuator; an accelerometer sensor was also used to validate the effectiveness of the PVDF. Three natural frequencies were chosen for excitation purposes and two ratios of them (1/2 and 1/3), which gives six tested frequency. The excitation was a sinus with an amplitude of 1 V. Several plates with different damages (delamination (35×35 mm^2), fiber cutting (70 mm), and holes (from 1.5 to 10 mm diameter)) were tested (Figure 33). The comparison of the amplitude of the sub- and super-harmonics was used as a damage indicator and showed sensitivity to detecting all of the introduced damages.

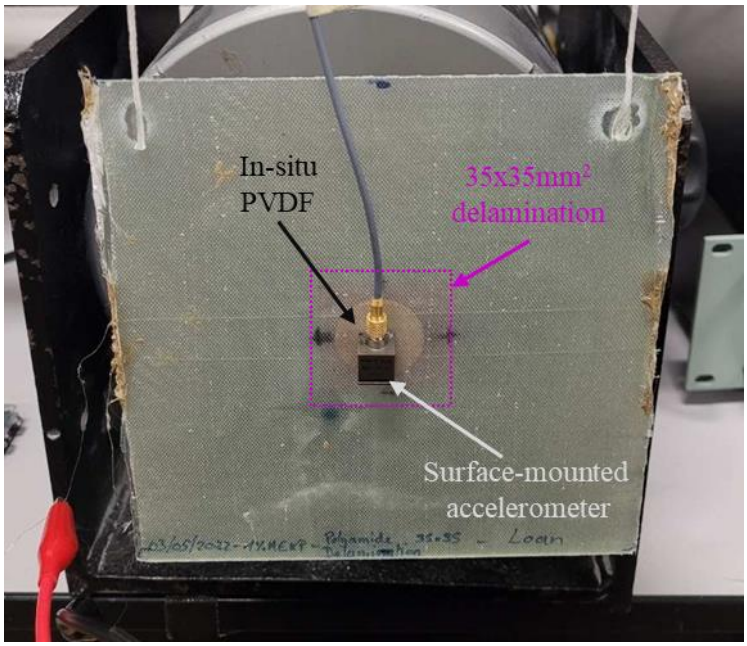

Figure 33. PMC plate used to perform the nonlinear vibration analysis. Delamination is introduced in the center of the plate. PVDF and accelerometer are used as sensors [122].

A similar technique was used in [123], named Second-harmonic generation, on a carbon/epoxy plate damaged from impact (at low (18 mm length) and high (32 mm length) energy) or 2 Teflon-FEP ($5 \times 5 \times 0.012$ or $10 \times 10 \times 0.012$ mm^3) insertion (Figure 34). The excitation was introduced from an in situ PZT with a sweep signal and a frequency band from 20 to 500 kHz. The goal was to determine which frequencies show the higher amplitudes of the output signal, and these frequencies became the input frequencies of the tests. Then, a signal with different amplitude from 60 to 100 V was sent, and vibration from an acoustic sensor on the surface was measured. A second harmonic generation was observable for the damaged plate. Similar experimentation with an LV was conducted in order to see if the chosen frequency was correct. In [124], a damage localization method was created based on the amplitude of the second harmonic generation and a network of surface-bonded PZTs. A nonlinear parameter is calculated as $\beta = \frac{A_{2fs}}{(A_{fs}{}^2)\, L_{ij}}$ (A_{2fs} and A_{fs} are the amplitudes of the second and the first harmonics; L_{ij} is the distance of the path). For every path of the network (actuator/sensor path), the one with the highest value of this parameter becomes the 'damaged path', and a map can be created to visualize the expected localization. This method showed nice results to localize damage with an error from 4 mm to 22 mm.

Another technique quite similar to the SFE was used in [120] with the same equipment as the SFE method. Instead of using a harmonic signal, this one used a sweep signal excitation, and the higher-harmonics band was observed for a damaged structure (Figure 35).

Table 9 summarizes other studies that have used the SFE method for the SHM of PMC materials.

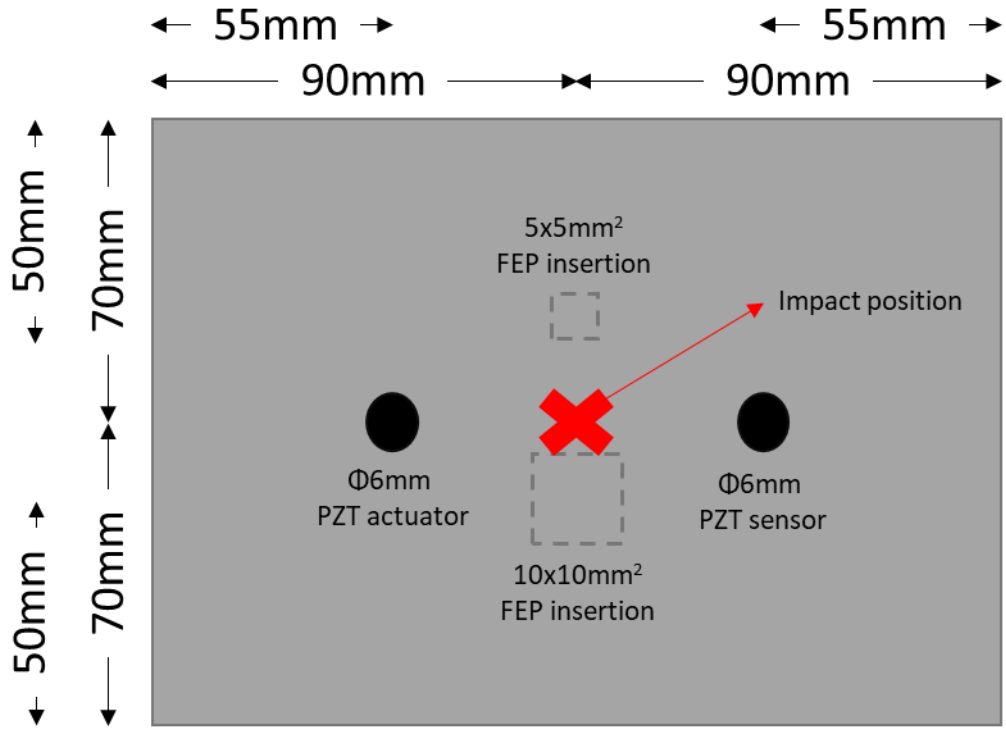

Figure 34. Specimen and damage specification (adapted from [123]).

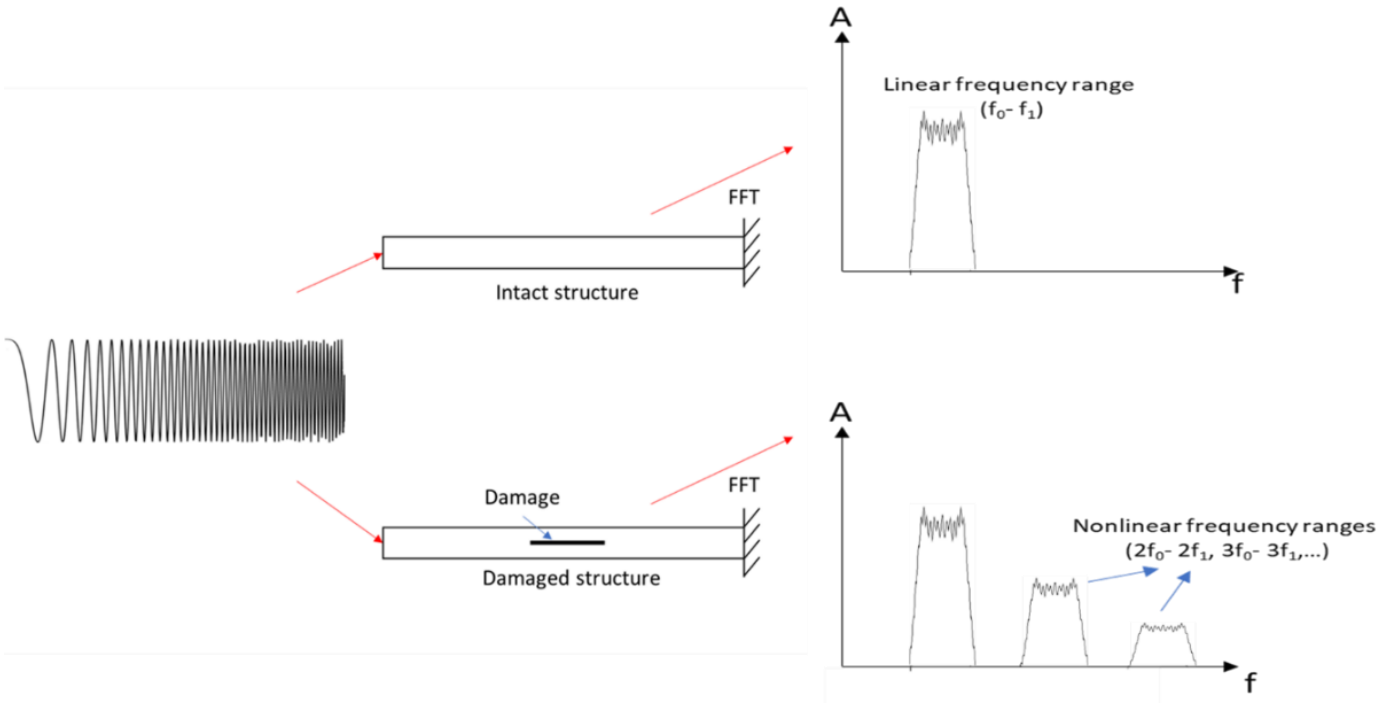

Figure 35. Schematic of the SWP method (adapted from [120]).

Table 9. Other articles about Single Frequency Excitation for SHM of PMC materials.

Method	Structure	Fixation	Input	Output	Damage	Description	Ref.
Higher harmonics	Carbon/epoxy-laminated plates	-	Signal generator Power amplifier Periodic signal	Accelerometer	BVID	Higher harmonics are observable and their amplitudes get bigger with higher damage severity	[125]

Table 9. *Cont.*

Method	Structure	Fixation	Input	Output	Damage	Description	Ref.
Damage indicator based on the amplitude of higher harmonics	Carbon/epoxy-laminated beam	Suspended with nylon cords	PI PL055.31—piezo actuator Harmonic excitation—6 V—1580, 2860, and 3915 Hz	PZT Oscilloscope	Impact damage	The first thing observed is that the response of the sensor is a linear function of the excitation amplitude for the intact structure, and this is not the case for the damaged ones. The damage index for the first frequency clearly detected the damage presence, but it was not the case for the two other frequencies. This is why they used a damage index combining all of the frequencies	[126]
Sub- and super-harmonics Velocity and acceleration distortions Phase portraits	Skin-stiffener composite structure	Freely suspended by elastic wire	Electromechanical shaker Single tone harmonic excitation signal—4th bending mode frequency—at different amplitude of excitation	LV	Damaged from impact testing (delamination)	Super-harmonics were present for the damaged structure Velocity, acceleration and also phase portrait showed distortion in the time-domain for damaged structure. Link between the motion of the structure and the distortions has been made. Opening and closing phases did not give high distortions, but the contact phase gave these distortions	[127]
Scaling subtraction method (SSM)	Carbon-fiber-reinforced polymer	Freely suspended by elastic ropes	Piezoelectric ceramic	LV	Far-end delamination	SSM methods showed very good results to filter noise and to effectively localize the delamination	[128]

4.2.2. Frequency Shifts from Different Excitation Amplitude

This technique consists of finding the natural frequencies of an intact and damaged structure for several amplitudes of excitation (for example, from 0.1 to 1 V every 0.1 V step). The frequency will be the same for an intact structure, while a loss of frequency will be observed for a damaged structure (Figure 36). The classical linear frequency shift can be observed between intact and damaged structures, but only the slope of decreasing frequency is used.

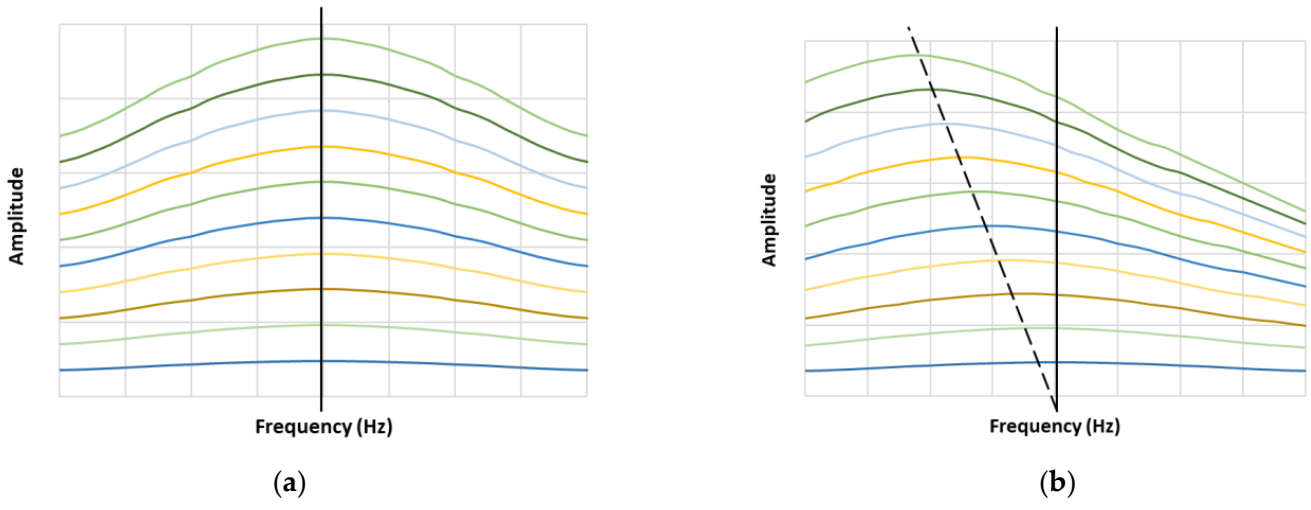

(**a**) (**b**)

Figure 36. Frequency shift for several amplitudes of excitation for intact (**a**) and damaged (**b**) structure.

In [66–68], this method was used on the same equipment as previously seen. A small frequency shift was present for intact beams and a big one for damaged beams. By using the elastic nonlinear parameter:

$$\alpha_f = -\frac{1}{\varepsilon}\left(\frac{f - f_0}{f_0}\right) \tag{18}$$

(f and f_0 are the current and the initial frequencies, ε is the strain), a higher sensitivity was shown compared to the linear natural frequency change (Figure 37). It reduces linearly as a function of the excitation amplitude.

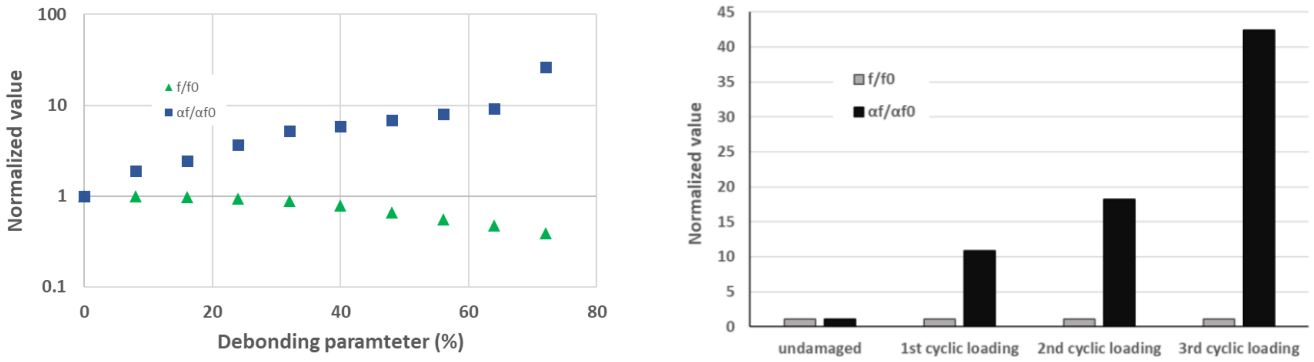

(**a**) (**b**)

Figure 37. Nonlinear elastic parameter sensibility against the linear frequency loss parameter: debonding on sandwich (**a**) (adapted from [67]) and fatigue damage induced on laminate (**b**) (adapted from [66]).

Another name for this method is the single-mode nonlinear resonance ultrasound (NRUS). In [129], several low-velocity impact damages (10 J with different sizes of impactors) were detected in carbon/epoxy plates. The excitation was a sweep signal around the first bending natural frequency; several experimentations were conducted by varying the amplitude of excitation. To visualize the delamination area (between 2.9 and 3.9 cm^2), a C-scan was used, and then the delamination area function of the nonlinear parameter α showed that this parameter is highly sensitive to damage area (Figure 38). In [130], the limits of the techniques in the previous article were investigated. A clamped carbon/epoxy plate was used with a speaker and an accelerometer. To investigate the influence of the clamping system on this method, the clamping setup was two steel plates with a torque system. By modifying the torque value, a frequency shift that increased while the torque value increased was observable; this directly means that the presence of a frequency shift is not only caused by damage but also by boundary conditions. This phenomenon can give false alarms about damage detection or hide them. For this, special care has to be taken when using it.

In [131], the "fast dynamic" and "slow dynamic" were investigated on concrete and composite materials. The fast dynamic is the successive measurement of resonant curves with different amplitudes of excitation without time between two excitations to avoid the material relaxing. The slow dynamic starts with the highest excitation and is kept for several minutes to "condition" the material. Then, the excitation is stopped, allowing the material to relax. To follow this relaxation, a low-excitation amplitude is introduced into the material, which permits following the evolution of the resonant curve in time. In this thesis, it is shown that the phenomenon of frequency shifts from different excitation amplitudes is induced by the conditioning and relaxing phenomena of the material. The fast dynamic on PMC was studied by focusing around the sixth bending mode with a frequency of 16.685 kHz and an amplitude varying from 10 to 100 mV amplified with a 52 dB gain. PZT patches as the actuator and sensor were used, and low damages with a

three-point bending test were gradually introduced in four steps. Then, with the same equipment, the slow dynamic was studied by using the 100 mV excitation. The conditioning process was first analyzed, and by letting the structure relax, the times of conditioning and relaxation were analyzed. By focusing on the time of relaxation, it was shown that this is a promising damage indicator for SHM; it seems that the damaged structure will have a lower natural frequency (linear method) but also that the damaged structure will relax to an initial frequency slower than an intact structure (Figure 39).

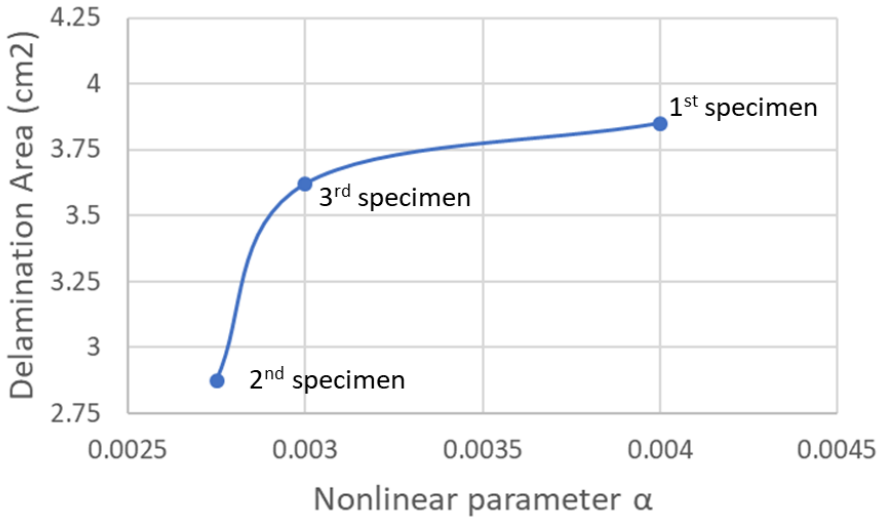

Figure 38. Delamination area function of the nonlinear parameter (adapted from [129]).

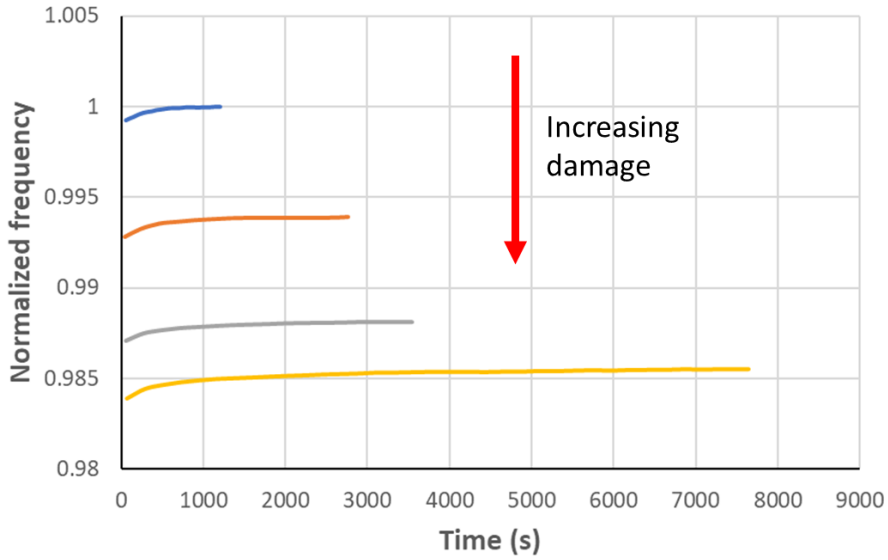

Figure 39. Time of relaxation of 4 damage levels of a PMC structure (adapted from [131]).

In [122], in addition to the SFE method, the NLR was also performed with the same configuration, damages, and equipment (Figure 33). Six natural frequencies were chosen for the excitation. The fiber cutting showed the biggest sensitivity in this method, with a big frequency shift for two tested modes, the delaminations showed a small sensitivity for one mode, and the holes showed sensitivity on five modes, with increasing frequency shift according to the increasing diameter of the hole.

Table 10 presents other studies using frequency shifts from different amplitudes of excitation methods for the SHM of the PMC materials.

Table 10. Other articles about frequency shifts from the different amplitudes of excitation methods for SHM.

Structure	Fixation	Input	Output	Damage	Description	Ref
CFRP-laminated plate	Supported by foam	Waveform generator Amplifier Speaker—100 Hz sweep signal around resonance frequencies—from 1.05 to 1.3 V (0.05 V step)	Accelerometer	Pendulum impact damage (repeated)	An obvious frequency shift is observable with increasing excitation amplitude. The damage indicator used in this article increased with the increase in the damage.	[132]
Rectangular beam of fibre-cemented slate	Suspended with nylon wires	Function generator Speaker Excited at the lowest flexural resonance mode at different amplitude	Accelerometer Labview	Hydrothermal shocks	The micro-cracks, induced by the hydrothermal shocks, clearly exhibited nonlinear behavior in the vibration response of the structure, with a frequency shift increasing with the damage severity.	[133]
Steel–TiC composite beams Glass rods Polymer-based beams		PZT or electromagnetic shaker Swept-sine signal—around bending mode frequencies—from 1 to 10 V	Accelerometer	Damage from tensile test	The classical nonlinear frequency shift gave nice results, but it was also combined with the harmonic-generation method, which showed higher sensitivity.	[134]
Flax/elium cross-ply and unidirectional composite	Clamped–Free	Impact hammer Shaker	LV Accelerometer	Damage from tensile test	Greater sensitivity obtained from the nonlinear resonance methods over the linear ones.	[135]

4.2.3. Vibro-Acoustic Modulation—VAM

The VAM methods may be beyond the scope of this article because some of the excitation frequencies used are in the ultrasonic field (ultrasound starts around 15~20 kHz). However, this is an interesting technique. It consists of exciting the structure with a pumping signal having a low frequency and applying a probing signal simultaneously with a high frequency; both excitations are harmonic signals. The nonlinearities caused by damage will induce super-harmonics of the pumping signal frequency (similar to the SFE method) and sub- and super-harmonics made of both "frequencies" modulation (also called sidebands) (Figure 40). This technique can have several names regarding the frequencies used: vibroacoustic modulation, Vibro-ultrasonic, etc. If pumping and probing frequencies are both very high, it will enter the ultrasonic field more than the vibration one. In most cases, the pumping frequency corresponds to the natural frequency of the structure, while the probing frequency is much higher (ultrasound). The reference [136] gives a small overview of this technique.

A lot of articles used the amplitude of this sideband as a damage indicator by comparing them with the sidebands of an intact structure (which should be very low). A similar technique is the Impact Modulation; this one uses an impact as the pumping excitation and an actuator as probing excitation. Wave distortions in the time domain (velocity, acceleration, voltage) can also be observed by performing VAM methods.

Some researchers name it the Nonlinear Wave Modulation Technique (NWMS). In [129], NWMS was used with two natural frequencies of carbon/epoxy plate (200 Hz and 2245 Hz). Damage in the plate was introduced through low-velocity impact, and the excitation of the structure was performed with a loudspeaker. Unfortunately, we do not have information about the sensing equipment (the accelerometer is the most commonly used). The results clearly showed the super-harmonics after the pumping frequency and the sidebands

around the probing frequency for the damaged structure. When the damage severity is elevated, the sideband amplitude is higher.

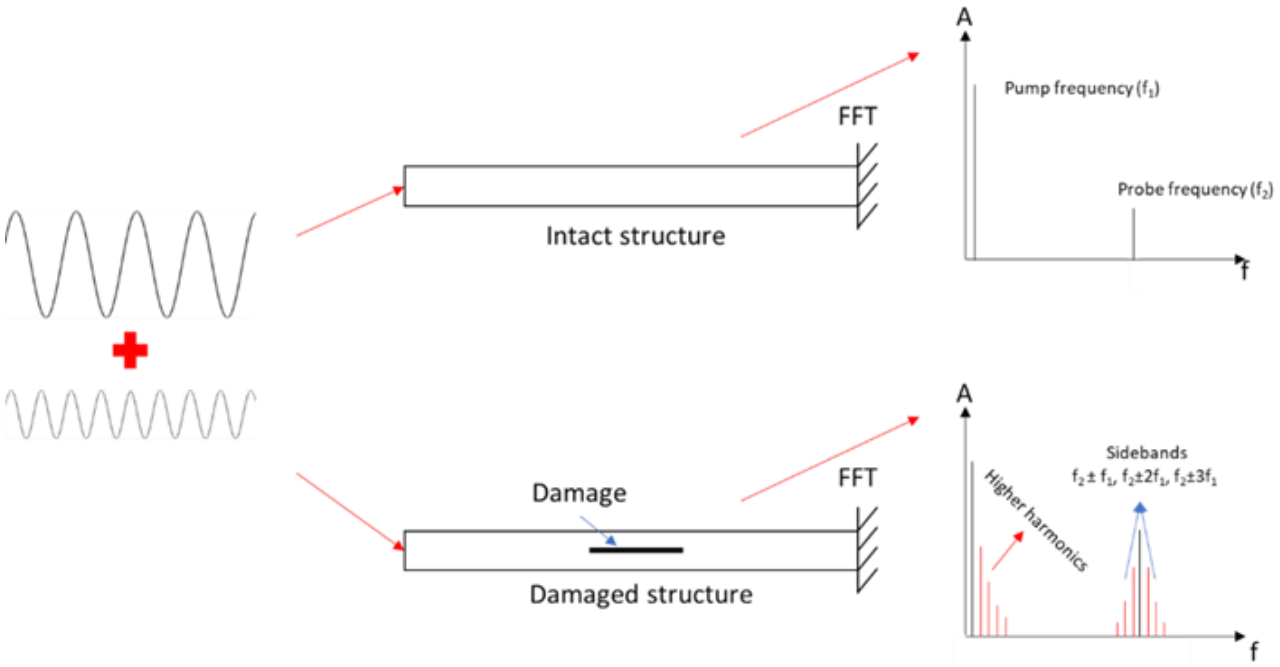

Figure 40. Schematic of the VAM method (adapted from [120]).

In [137], the VAM method was used with two in situ PZTs as actuators and one acoustic sensor on the surface of a carbon/epoxy plate. The setup was the same as with the SFE method. One PZT was excited with a harmonic signal at 18 kHz and another one at 192 kHz (these values were obtained after finding the best combination that generates higher modulation). Sidebands were observable only for the damaged plates, and they confirmed this with LV experimentation. In [130], the limits of VAM methods were also investigated. The same configuration as previously seen with the SFE method was used, with the carbon/epoxy plate clamped between two steel plates with different torque values. Higher harmonics and sidebands for undamaged structures were observable, and the higher the torque value, the higher the amplitude of harmonics and sidebands. This means that false damage detection can happen while performing this method, and we should be careful about the boundary condition.

As we have seen through these articles, the choice of the best combination of frequencies is important to increase the accuracy of the method. This is why in [138] this choice was investigated through several experimentations on carbon/epoxy plates with impact damage. First, a classical modal analysis with an electromagnetic shaker using white noise and LV was performed in order to choose the best natural frequencies for the VAM method. Secondly, the high-frequency sinusoidal signal with a piezoelectric transducer and the low-frequency signal with the electromagnetic shaker were sent to the structure. The two natural frequencies previously determined were used for the low-frequency excitation, while Local Defect Resonance (LDR—[139–141]) and a random high frequency were used for the probing signal. The results obtained from an LV showed that the combination with higher sensitivity is to use a natural frequency corresponding to a mode with an out-of-plane motion as a pumping signal and the LDR as a probing signal.

In [120], the vibration was introduced with PZT in a carbon/epoxy plate with delamination created from Teflon-FEP insertion. The pumping signal had a 5 kHz frequency, and the probing signal had a 100 kHz frequency. Then, the pumping and the probing frequency were changed sequentially. In order to evaluate the influence of each frequency, a damage index calculated from the amplitude of the sidebands was used.

In [142,143], this technique was investigated with surface-bonded PZTs, and especially its limitations. On a carbon/epoxy plate, with impact damage in a cantilever configuration, the clamping conditions affected the amplitude of sidebands for undamaged structures, as previously seen, but also for damaged structures. Similarly, with a lot of articles, the sidebands happened around the probing frequency for damaged cases but also for undamaged cases. Then, the observation that the amplitude of fundamental increases, while clamping force is increasing for undamaged plates, was made, and it is the reverse for the damaged ones. Otherwise, the amplitude of sidebands decreases while the clamping force increases for undamaged plates, and it is the reverse for damaged ones (Figure 41).

When clamping force ↗	Undamaged	Damaged (10J impact)
Fundamental amplitude	↗	↘
Sidebands amplitude	↘	↗

Figure 41. Effect of increasing clamping force on fundamental and sidebands amplitude for the undamaged and damaged plate: ↗ and ↘ mean increasing and decreasing (adapted from [142]).

In [144], the same structure as in [127,145], the skin-stiffener composite one, was used with the VAM method. This structure was damaged through impact testing, which mainly created delamination. A shaker was used to introduce the pumping signal with a frequency of 1455 Hz and a piezoelectric diaphragm was used to introduce the probing one with a frequency of 50 kHz. Then, the vibration was caught by an LV. By using a Hilbert Transform, instantaneous amplitude and frequency were obtained and used to plot them over time. Two damage indicators represented by the peak-to-peak value of the signal were used, and their distributions over the length of the structure showed that the instantaneous amplitude has high sensitivity in the area of the damage; this is not the case for instantaneous frequency.

In [146,147], both probing and pumping signals were sent to the same actuator, which is an interesting way of using this technique.

Table 11 presents other studies using the VAM method for the SHM purposes of PMC materials.

4.2.4. Damping

According to [104], damping can also have nonlinear features. One is called the instantaneous damping coefficient, and the other is the nonlinear damping parameter.

The instantaneous damping coefficient is determined from Continuous Wavelet Transform (CWT) on the vibration response of the structure; it was created to show the variation of damping over time. The instantaneous amplitude and phase are extracted from the CWT to create the instantaneous damping coefficient h_0.

$$h_0(t) = -\frac{\dot{A}}{A} - \frac{\dot{\omega}}{2\omega} \tag{19}$$

where A is the instantaneous amplitude and ω is the damped angular frequency, with their first derivative.

The nonlinear damping parameter α_Q, also known as the dissipative nonlinear parameter, can be found using the same method as "frequency shift with different amplitude of excitation". Indeed, the dissipative parameter can be calculated from [66,67]:

$$\alpha_Q = \frac{1}{\varepsilon}\left(\frac{1}{Q} - \frac{1}{Q_0}\right) \tag{20}$$

where Q is the loss quality factor (1/loss factor), Q_0 is the loss of quality factor for the first low amplitude, and ε is the strain.

Table 11. Other articles about the VAM method for SHM.

Structure	Fixation	Input	Frequencies	Output	Damage	Description	Ref.
Carbon/epoxy-laminated beam	Glued on an aluminum stud linked to the rod of the shaker	Pump: • Generator (Agilent 3200 A)—Sinusoidal—0.5 to 2 V • Shaker Probe: • Generator (TTi TG2000)—Sinus 20 V • PZT	Pump: 155, 282 and 494 Hz Probe: 6710 and 7180 Hz	Accelerometer	Delamination and fiber break (impact damage at 1.8 and 2.4 J)	VAM clearly detected damage occurrence in composite beam, but the accuracy of it depends on the choice of the pumping and probing frequencies. The lowest pumping frequency showed higher performance.	[148]
Carbon-reinforced fiberglass wind turbine	On service	Pump: • Rotational speed of the rotor • Impact • PCB Piezotronics disk Probe: • 9 V-battery and power amplifier—Sinusoidal • MFC	Pump: 3.1, 6.2, 9.4, 400 Hz Probe: 5–10 kHz	MFC	Crack	VAM can be used while the turbine is rotating, and it can detect the presence of damage. The sidebands for damage cases were higher than for the healthy structure, but it still showed high sidebands for the healthy structure.	[149]
CFRP	Fix-end	Pump: • Surface-bonded piezoceramic • Voltage amplifier WMA-300 Probe: • Instron 8802L2741	Pump: 3 Hz Probe: 185–220 kHz	Surface-bonded piezoceramic	Hole	The pump wave for VAM was created from a fatigue mechanical loading, which is an original way. Phase modulation showed higher sensitivity than frequency modulation.	[150]

In [66,67], the dissipative parameter was used to evaluate its sensibility to damage against the classical loss factor. The configuration was the same as for the elastic parameter on the sandwich and the laminate. A higher sensibility of this dissipative nonlinear parameter over the linear one was found (Figure 42). This behavior was also been investigated in [134], where the dissipative parameter showed a high sensitivity for damaged cases.

4.3. Summary of the Vibration Methods and Decision Tree

Many methods have been presented, and most of the researchers investigated several of them in their articles. For example, the natural frequencies shift is often combined with the damping ratio and the modes shape methods: modes shapes, modes shape curvature, modal strain energy, and modal flexibility (as in Figure 22). These three methods linked to modes shape need only to be calculated, but it would not be wise not to use them. In addition, for all of the methods, a general overview of the vibration of the structure over a large frequency band is needed. From this result, the natural frequencies and the damping ratio only have to be detected and calculated, and this is why they are always used as a first reference. In nonlinear methods, the sub- and super-harmonics generation induced by damage is also often investigated through SFE and VAM in the same articles. Indeed, the techniques are a bit different, but the phenomena observed are similar. These two techniques are both vibro-ultrasonic methods, where the frequencies used for excitation

can either correspond to the modes of vibration or ultrasonic wave, but both showed that they can be used within the vibration field efficiently.

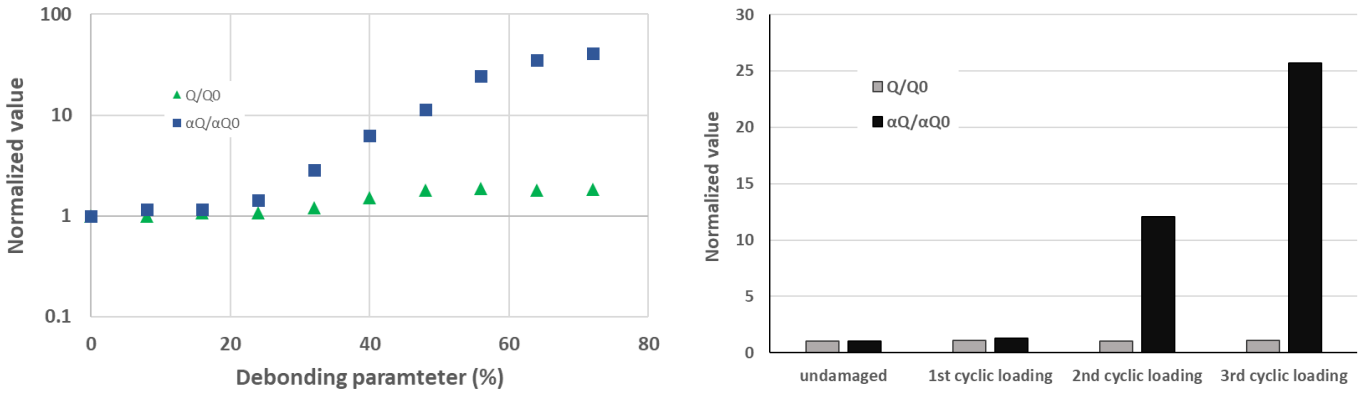

(**a**) (**b**)

Figure 42. Nonlinear dissipative parameter sensibility against the linear loss factor parameter: debonding on a sandwich (**a**) (adapted from [67]) and fatigue damage induced on the laminate (**b**) (adapted from [66]).

In Tables 12 and 13, a summary of the linear and nonlinear techniques is given, as well as the accuracy of each method for specific damages (these tables are built from the cited article). This review helped to build a decision tree about the SHM of PMC performing vibration analysis (Figure 43).

Table 12. Linear vibration methods for SHM (Detected Size represents the minimum percentage of the detected damaged area divided by the total area).

Technique	What Is Needed?	How to?	Drawbacks	Damage	Detected Size
Natural frequencies shift	The vibration of the structure in the frequency domain for a large frequency range is needed to evaluate the natural frequencies.	Send a white noise or a sweep signal with a large frequency band. Compare the natural frequencies of intact and damaged structures.	Only big damages are detectable. It can be influenced by some external conditions: temperature, boundary conditions, etc. Some modes show a higher shift, which means several modes have to be tested.	Delamination	>20%
				Crack	>20%
				Impact	X
				Fiber cutting	X
				Debonding	>16%
Modes shape (MS)	The vibration of the structure in the frequency domain for a large frequency range and at several locations is needed to record the mode shapes.	With LV, a network of sensors, or a roving input method, displacement at several locations can be obtained. Several criteria comparing intact and damaged structures can be used: MAC, CoMAC, ECoMAC, PrMAC, etc.	A large number of sensors or heavy processes are needed.	Delamination	>10%
				Crack	>10%
				Impact	>10%
				Layer cutting	>0.4%
Mode shape curvature	The modes shape.	Several criteria comparing intact and damaged structures can be used: MSC, NMSC, NCDF, etc.		Crack	>27.7%
				Surface cut	>7%
				Debonding	>10%
Modal strain energy	The modes shape.	Several criteria comparing intact and damaged structures can be used: MSEC, MSED, CMSE, etc.		Delamination	>11%
				Surface cut	>11%
				Impact	>11%
				Debonding	>1.2%
Modal flexibility	The modes shape.	Check the flexibility change.		Core	>0.3%

Table 12. *Cont.*

Technique	What Is Needed?	How to?	Drawbacks	Damage	Detected Size
Damping	The vibration of the structure is needed, and the damping can be obtained with several techniques, but the most classical one is the −3 dB method.	Send a white noise or a sweep signal with a large frequency band. Compare the damping parameter of intact and damaged structures.	Mainly influenced by operational factors and uncertainty in the damping characterization.	Delamination	>48%
				Fatigue	3rd cycle
				Impact	BVID
FRF	Input and output are needed to build the FRF.	Some metrics can be used to observe differences in the FRF of intact and damaged structures for a large frequency range.		Impact	
				Hole	
TF	The displacements or velocities at several locations of the structure for the same input are needed.	A ratio of two displacements or velocities has to be made, and a damage indicator is calculated from this ratio.	A large number of sensors or heavy processes are needed.	Bonding steel plate	>20%
				Impact	>5 J
WT	Vibration output in the time domain.	The general vibration of the structure is needed, and the time domain signal should be divided into several sub-signals to compare each sub-signal energy.	Extra processing is needed, and the correct choice of wavelets should be made.	Delamination	>0.12%

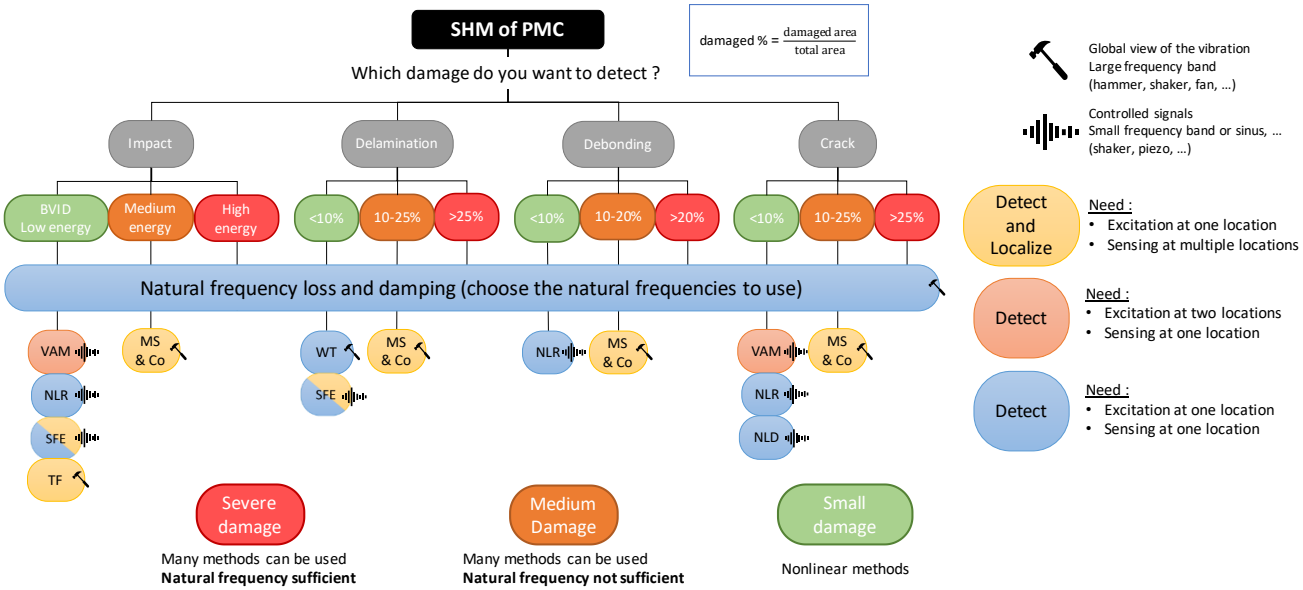

Figure 43. Decision tree of vibration methods for specific damage in PMC structure.

Table 13. Nonlinear vibration methods for SHM (Detected Size represents the minimum percentage of the detected damaged area divided by the total area).

Technique	What Is Needed?	How to?	Drawbacks	Damage	Detected Size
SFE	Global knowledge of the vibration of the structure to choose the best frequency for the harmonic signal excitation.	Compare damaged and intact structures through distortions in time-domain and phase portraits, sub- and super-harmonics, and damage indicators.	Small peaks can be hidden in the noise in operational detection.	Impact	BVID (>7 J)
				Delamination	>3%
Nonlinear resonance (NLR) and damping	Global knowledge of the vibration of the structure to choose the natural frequencies used for this technique with a harmonic or a sweep signal around these frequencies.	Compare the resonance curves obtained from different amplitudes of excitation for damaged and intact structures. Use nonlinear elastic and dissipative parameters as damage indicators.	A lot of tests have to be performed to obtain the resonance curves (10 in general) for 1 natural frequency. The frequency shift is also influenced by the boundary condition.	Debonding	>8%
				Fatigue crack	1st cycle
				Impact	BVID (10 J and 2400 times 3 J)

Table 13. *Cont.*

Technique	What Is Needed?	How to?	Drawbacks	Damage	Detected Size
VAM	Global knowledge of the vibration of the structure to choose the best frequency of excitation for the pumping signal and, in some cases, also for probing one.	Compare the occurrence of super-harmonics and sidebands between damaged and intact structures. Damage indicators based on their amplitude are also used.	This method is influenced a lot by the boundary conditions, so special care should be made with VAM.	Impact	BVID (>1.8 J)
				Crack	
Nonlinear Damping (NLD)	Time-frequency domain signal is needed in order to perform the CWT.	Extract the instantaneous amplitude and phase of the response to calculate the instantaneous damping. Compare the variation of it between intact and damaged structures.	Post-processing techniques (CWT) have to be used to obtain the instantaneous parameters, which are necessary for the damping calculation.	Delamination	>32%
				Fatigue crack	2nd cycle

5. Conclusions

An important amount of techniques and the main methods of vibration analysis for SHM have been presented in this article, with a focus on PMC materials. The goal of this review was to study the techniques, used equipment, and configurations, as well as their effectiveness and, for some techniques, their drawbacks and limitations. We also reviewed the different damage mechanisms detected or not with these techniques, which allows for selecting the best method according to the studied damage.

Firstly, the classical linear methods have been introduced, even though they are considered insufficient to detect small and complex damage in the composite structures, and secondly, the nonlinear methods have shown interesting capacities in the last few years in detecting and locating damage with nonlinear behavior of the structure. The nonlinear methods are still in development, and nowadays there already exist three main techniques that can easily be used to perform SHM of PMC: the SFE, the VAM, and the nonlinear resonance.

This review highlighted the possibility of using vibration analysis for SHM of PMC. However, some limitations have been observed, such as relatively low sensitivity to early-stage damage, environmental effects, optimal sensor position, signal processing, etc. In the introduction, the concept of SHM has been presented, and from the cited articles, it is clear that the step of qualifying the damage mechanism is not yet well-developed in vibration analysis, whereas detection and localization are possible through several techniques. This indicates that further advancements are needed in this field, whether through the development of more optimized and/or internal sensors within the structure (smart materials), improved signal processing, or the development of new vibration analysis methods. A growing interest in Artificial Intelligence (AI) [151] has showed promising potential in the context of data processing in SHM and vibration analysis. This could become a significant asset for advancing the qualification aspect of SHM by enabling real-time data interpretation and adaptive damage detection strategies and thus providing a more robust and automated assessment of service life estimation. In addition, most of them investigated the presence of damage on laboratory-scale composite structures. This is important to take into consideration as the transposition to the operational scale still needs improvement and development.

To counteract these limitations for SHM diagnostics, current studies focus on combining the results of several vibration methods and also with other NDT results (such as AE, US, etc.). Indeed, this combination permits us to obtain a multi-sources and multi-physics response of the structure, thus enhancing the diagnostics. Indeed, a large range of NDT exists, which allows for combining them and obtaining different information about the damaged structure. Here, the AI algorithms have also demonstrated that they can become a major element in this combination in order to visualize similar patterns induced by the different types of damage through all of these techniques. This will help to avoid fake detec-

tion/localization and to increase accuracy in the SHM process, with the goal of qualifying the damage mechanisms efficiently.

Author Contributions: Conceptualization, W.H., Z.A. and L.D.; methodology, W.H., Z.A. and L.D.; formal analysis, W.H. and L.D.; investigation, W.H. and L.D.; data curation, L.D.; writing—original draft preparation, W.H. and L.D.; writing—review and editing, W.H., Z.A. and L.D.; supervision, W.H., Z.A. and L.D.; project administration, W.H. and Z.A.; funding acquisition, W.H. All authors have read and agreed to the published version of the manuscript.

Funding: The authors would like to thank the Ministère de l'Enseignement Supérieur et de la Recherche of France for funding this work as part of the doctoral thesis of Loan Dolbachian. This research was funded by Ministère de l'Enseignement Supérieur et de la Recherche of France.

Data Availability Statement: The raw/processed data required to reproduce these findings cannot be shared at this time as the data also form part of an ongoing study.

Conflicts of Interest: The authors declare no conflicts of interest.

Glossary

AE	Acoustic Emission
AI	Artificial Intelligence
BVID	Barely Visible Impact Damage
CFRP	Carbon-Fiber Reinforced Polymer
CMC	Ceramic-Matrix Composite
DaDI	Damping Damage Indicator
DI	Damage Indicator
DIC	Digital Image Correlation
FEP	Fluorinated Ethylene Propylene
FFT	Fast Fourier Transform
FRF	Frequency Response Function
GFRP	Glass-Fiber-Reinforced Polymer
LDR	Local Defect Resonance
LV	Laser Vibrometer
MAC	Modal Assurance Criterion
MF	Modal Flexibility
MFC	Macro-Fiber Composite
MMC	Metal-Matrix Composite
MSC	Modal Shape Curvature
MSD	Modal Shape Displacement
MSE	Modal Strain Energy
NDT	Non-Destructive Techniques
NWMS	Nonlinear Wave Modulation Technique
PFC	Piezo-Fiber Composite
PM	Process Monitoring
PMC	Polymer-Matrix Composite
PSF	Plane Shape Function
PVC	PolyVinyl Chloride
PVDF	Polyvinylidene Fluoride
PZT	Lead Zirconate Titanate
SFE	Single Frequency Excitation
SHM	Structural Health Monitoring
SWP	Sweep Signal Excitation
TF	Transmittance or Transmissibility Function
UT	Ultrasonic Testing
VAM	Vibro-Acoustic Modulation

References

1. Harizi, W.; Chaki, S.; Bourse, G.; Ourak, M. Mechanical Damage Characterization of Glass Fiber-Reinforced Polymer Laminates by Ultrasonic Maps. *Compos. B Eng.* **2015**, *70*, 131–137. [CrossRef]
2. Harizi, W.; Chaki, S.; Bourse, G.; Ourak, M. Mechanical Damage Assessment of Polymer-Matrix Composites Using Active Infrared Thermography. *Compos. B Eng.* **2014**, *66*, 204–209. [CrossRef]
3. Harizi, W.; Chaki, S.; Bourse, G.; Ourak, M. Mechanical Damage Assessment of Glass Fiber-Reinforced Polymer Composites Using Passive Infrared Thermography. *Compos. B Eng.* **2014**, *59*, 74–79. [CrossRef]
4. Saba, N.; Jawaid, M. A Review on Thermomechanical Properties of Polymers and Fibers Reinforced Polymer Composites. *J. Ind. Eng. Chem.* **2018**, *67*, 1–11. [CrossRef]
5. Al-Haik, M.S.; Hussaini, M.Y.; Garmestani, H. Prediction of Nonlinear Viscoelastic Behavior of Polymeric Composites Using an Artificial Neural Network. *Int. J. Plast.* **2006**, *22*, 1367–1392. [CrossRef]
6. Sajan, S.; Philip Selvaraj, D. A Review on Polymer Matrix Composite Materials and Their Applications. *Mater. Today Proc.* **2021**, *47*, 5493–5498. [CrossRef]
7. Jia, Z.; Li, T.; Chiang, F.P.; Wang, L. An Experimental Investigation of the Temperature Effect on the Mechanics of Carbon Fiber Reinforced Polymer Composites. *Compos. Sci. Technol.* **2018**, *154*, 53–63. [CrossRef]
8. Indra Reddy, M.; Vijaya Kumar Raju, P.; Bhargava, N.R.M.R. Experimental Investigation on the Mechanical and Thermal Properties of Sprouts Center Stem (Asian Palmyra) Fiber Reinforced Polymer Composites. *Mater. Today Proc.* **2018**, *5*, 7808–7817. [CrossRef]
9. Colombo, C.; Vergani, L.; Burman, M. Static and Fatigue Characterisation of New Basalt Fibre Reinforced Composites. *Compos. Struct.* **2012**, *94*, 1165–1174. [CrossRef]
10. Harizi, W.; Chaki, S.; Ourak, M.; Harizi, W.; Chaki, S.; Bourse, G.; Ourak, M. Characterization of the Damage Mechanisms in Polymer Composite Materials by Ultrasonic Waves, Acoustic Emission and Infrared Thermography. In Proceedings of the ECCM15, Venice, Italy, 24–28 June 2012.
11. Rytter, A. Vibrational Based Inspection of Civil Engineering Structures. *Fract. Dyn.* **1993**, *R9314*, 44.
12. Jones, D.R.H.; Ashby, M.F. *Engineering Materials 1—An Introduction to Their Properties & Applications*; Butterworth-Heinemann: Oxford, UK, 1996.
13. Tuloup, C.; Harizi, W.; Aboura, Z.; Meyer, Y.; Khellil, K.; Lachat, R. On the Use of In-Situ Piezoelectric Sensors for the Manufacturing and Structural Health Monitoring of Polymer-Matrix Composites: A Literature Review. *Compos. Struct.* **2019**, *215*, 127–149. [CrossRef]
14. Bastianini, F.; di Tommaso, A.; Pascale, G. Ultrasonic Non-Destructive Assessment of Bonding Defects in Composite Structural Strengthenings. *Compos. Struct.* **2001**, *53*, 463–467. [CrossRef]
15. Aymerich, F.; Meili, S. Ultrasonic Evaluation of Matrix Damage in Impacted Composite Laminates. *Compos. B Eng.* **2000**, *31*, 1–6. [CrossRef]
16. Bourchak, M.; Farrow, I.R.; Bond, I.P.; Rowland, C.W.; Menan, F. Acoustic Emission Energy as a Fatigue Damage Parameter for CFRP Composites. *Int. J. Fatigue* **2007**, *29*, 457–470. [CrossRef]
17. Harizi, W.; Chaki, S.; Bourse, G.; Ourak, M. Damage Mechanisms Assessment of Glass Fiber-Reinforced Polymer (GFRP) Composites Using Multivariable Analysis Methods Applied to Acoustic Emission Data. *Compos. Struct.* **2022**, *289*, 115470. [CrossRef]
18. Hack, E.; Rastogi, P. *Optical Methods for Solid Mechanics*; Wiley: Hoboken, NJ, USA, 2012.
19. McCormick, N.; Lord, J. Digital Image Correlation. *Mater. Today* **2010**, *13*, 52–54. [CrossRef]
20. Schilling, P.J.; Karedla, B.P.R.; Tatiparthi, A.K.; Verges, M.A.; Herrington, P.D. X-ray Computed Microtomography of Internal Damage in Fiber Reinforced Polymer Matrix Composites. *Compos. Sci. Technol.* **2005**, *65*, 2071–2078. [CrossRef]
21. Wang, L.B.; Frost, J.D.; Voyiadjis, G.Z.; Harman, T.P. Quantification of Damage Parameters Using X-ray Tomography Images. *Mech. Mater.* **2003**, *35*, 777–790. [CrossRef]
22. Gaussorgues, G.S.C. *Infrared Thermography*; Springer: Berlin/Heidelberg, Germany, 1993.
23. Chaupal, P.; Rajendran, P. A Review on Recent Developments in Vibration-Based Damage Identification Methods for Laminated Composite Structures: 2010–2022. *Compos. Struct.* **2023**, *311*, 116809. [CrossRef]
24. Gomes, G.F.; Mendez, Y.A.D.; da Silva Lopes Alexandrino, P.; da Cunha, S.S.; Ancelotti, A.C. A Review of Vibration Based Inverse Methods for Damage Detection and Identification in Mechanical Structures Using Optimization Algorithms and ANN. *Arch. Comput. Methods Eng.* **2019**, *26*, 883–897. [CrossRef]
25. Bovsunovsky, A.; Surace, C. Non-Linearities in the Vibrations of Elastic Structures with a Closing Crack: A State of the Art Review. *Mech. Syst. Signal Process.* **2015**, *62*, 129–148. [CrossRef]
26. He, M.; Zhang, Z.; Ramakrishnan, K.R. Delamination Identification for FRP Composites with Emphasis on Frequency-Based Vibration Monitoring–A Review. *SDHM Struct. Durab. Health Monit.* **2018**, *12*, 213–256. [CrossRef]
27. Hou, R.; Xia, Y. Review on the New Development of Vibration-Based Damage Identification for Civil Engineering Structures: 2010–2019. *J. Sound. Vib.* **2021**, *491*, 115741. [CrossRef]
28. Montalvão, D.; Maia, N.M.M.; Ribeiro, A.M.R. A Review of Vibration-Based Structural Health Monitoring with Special Emphasis on Composite Materials. *Shock. Vib. Dig.* **2006**, *38*, 295–324. [CrossRef]

29. Sinou, J.-J. A Review of Damage Detection and Health Monitoring of Mechanical Systems from Changes in the Measurement of Linear and Non-Linear Vibrations. In *Mechanical Vibrations: Measurement, Effects and Control*; Nova Science: Hauppauge, NY, USA, 2013.
30. Worden, K.; Farrar, C.R.; Haywood, J.; Todd, M. A Review of Nonlinear Dynamics Applications to Structural Health Monitoring. *Struct. Control Health Monit.* **2008**, *15*, 540–567. [CrossRef]
31. Fan, W.; Qiao, P. Vibration-Based Damage Identification Methods: A Review and Comparative Study. *Struct. Health Monit.* **2011**, *10*, 83–111. [CrossRef]
32. Hassani, S.; Mousavi, M.; Gandomi, A.H. Structural Health Monitoring in Composite Structures: A Comprehensive Review. *Sensors* **2021**, *22*, 153. [CrossRef]
33. Akay, M. *An Introduction to Polymer-Matrix Composites*; Bookboon: London, UK, 2015; ISBN 9788740309805.
34. Tang, X.; Yan, X. A Review on the Damping Properties of Fiber Reinforced Polymer Composites. *J. Ind. Text.* **2020**, *49*, 693–721. [CrossRef]
35. Mohan Kumar, S.; Raghavendra Ravikiran, K.; Govindaraju, H.K. Development of E-Glass Woven Fabric/Polyester Resin Polymer Matrix Composite and Study of Mechanical Properties. *Mater. Today Proc.* **2018**, *5*, 13367–13374. [CrossRef]
36. Tableau, N.; Aboura, Z.; Khellil, K.; Laurin, F.; Schneider, J. Multiaxial Loading on a 3D Woven Carbon Fiber Reinforced Plastic Composite Using Tensile-Torsion Tests: Identification of the First Damage Envelope and Associated Damage Mechanisms. *Compos. Struct.* **2019**, *227*, 111305. [CrossRef]
37. Loi, G.; Marongiu, G.; Porcu, M.C.; Aymerich, F. Vibro-Acoustic Modulation with Broadband Pump Excitation for Efficient Impact Damage Detection in Composite Materials. *IOP Conf. Ser. Mater. Sci. Eng.* **2023**, *1275*, 012008. [CrossRef]
38. Talreja, R. PMC Failure Mechanisms. In *Comprehensive Composite Materials II*; Elsevier: Amsterdam, The Netherlands, 2017; pp. 107–117. [CrossRef]
39. Greenhalgh, E. Defects and Damage and Their Role in the Failure of Polymer Composites. In *Failure Analysis and Fractography of Polymer Composites*; Woodhead: Cambridge, UK, 2009; pp. 356–440. [CrossRef]
40. Duchene, P.; Chaki, S.; Ayadi, A.; Krawczak, P. A Review of Non-Destructive Techniques Used for Mechanical Damage Assessment in Polymer Composites. *J. Mater. Sci.* **2018**, *53*, 7915–7938. [CrossRef]
41. Bolotin, V. Mechanics of Delaminations in Laminate Composite Structures. In *Mechanics of Composite Materials*; CRC Press: Boca Raton, FL, USA, 2001; Volume 37.
42. Avitabile, P. Experimental modal analysis. *Sound Vib.* **2001**, *35*, 20–31.
43. Kranjc, T.; Slavić, J.; Boltežar, M. A Comparison of Strain and Classic Experimental Modal Analysis. *JVC J. Vib. Control.* **2016**, *22*, 371–381. [CrossRef]
44. Cugnoni, J.; Guzman, E.; Cugnoni, J.; Gmür, T. Use of PVDF Transducers as Actuators for Operational Modal Analysis on Composite Samples. In Proceedings of the ICCE21, Tenerife, Spain, 21–27 July 2013.
45. Guzman, E.; Cugnoni, J.; Gmur, T. Monitoring of Composite Structures Using a Network of Integrated PVDF Film Transducers. *Smart Mater. Struct.* **2015**, *24*, 055017. [CrossRef]
46. Xin, Y.; Sun, H.; Tian, H.; Guo, C.; Li, X.; Wang, S.; Wang, C. The Use of Polyvinylidene Fluoride (PVDF) Films as Sensors for Vibration Measurement: A Brief Review. *Ferroelectrics* **2016**, *502*, 28–42. [CrossRef]
47. Bregar, T.; Starc, B.; Čepon, G.; Boltežar, M. On the Use of PVDF Sensors for Experimental Modal Analysis. In *Proceedings of the Society for Experimental Mechanics Series*; Springer: Berlin/Heidelberg, Germany, 2021; pp. 279–281.
48. Tuloup, C.; Harizi, W.; Aboura, Z.; Meyer, Y.; Ade, B.; Khellil, K. Detection of the Key Steps during Liquid Resin Infusion Manufacturing of a Polymer-Matrix Composite Using an in-Situ Piezoelectric Sensor. *Mater. Today Commun.* **2020**, *24*, 101077. [CrossRef]
49. Janeliukstis, R.; Mironovs, D. Smart Composite Structures with Embedded Sensors for Load and Damage Monitoring–A Review. *Mech. Compos. Mater.* **2021**, *57*, 131–152. [CrossRef]
50. Paradies, R.; Ruge, M. In Situ Fabrication of Active Fibre Reinforced Structures with Integrated Piezoelectric Actuators. *Smart Mater. Struct.* **2000**, *9*, 220. [CrossRef]
51. Kovalovs, A.; Wesolowski, M.; Barkanov, E.; Gluhihs, S. Application of Macro-Fiber Composite (MFC) as a Piezoelectric Actuator. *Vibromech. J. Vibroeng.* **2009**, *11*, 105–112.
52. Siemens Company. What Is a Frequency Response Function (FRF)? Available online: https://community.sw.siemens.com/s/article/what-is-a-frequency-response-function-frf (accessed on 11 March 2022).
53. Siemens Company. Autopower Function. Available online: https://community.sw.siemens.com/s/article/the-autopower-function-demystified (accessed on 11 March 2022).
54. Baptiste Chomette MIMO Modal Parameters Identification in Frequency Domain–File Exchange–MATLAB Central. Available online: https://fr.mathworks.com/matlabcentral/fileexchange/82380-mimo-modal-parameters-identification-in-frequency-domain (accessed on 11 April 2022).
55. An, H.; Youn, B.D.; Kim, H.S. A Methodology for Sensor Number and Placement Optimization for Vibration-Based Damage Detection of Composite Structures under Model Uncertainty. *Compos. Struct.* **2022**, *279*, 114863. [CrossRef]
56. Mallardo, V.; Aliabadi, M.H. Optimal Sensor Placement for Structural, Damage and Impact Identification: A Review. *SDHM Struct. Durab. Health Monit.* **2014**, *9*, 287–323. [CrossRef]

57. Ferreira Gomes, G.; SimõesSim, S.; da Cunha, S., Jr.; da Silva Lopes Alexandrino, P.; Silva de Sousa, B.; Carlos Ancelotti Jr, A. Sensor Placement Optimization Applied to Laminated Composite Plates under Vibration. *Struct. Durab. Health Monit.* **2022**, *58*, 2099–2118. [CrossRef]
58. Doebling, S.W.; Farrar, C.R.; Prime, M.B.; Shevitz, D.W. Damage Identification and Health Monitoring of Structural and Mechanical Systems from Changes in Their Vibration Characteristics: A Literature Review. *Shock. Vib. Dig.* **1996**, *30*, 249299.
59. Lifshitz, J.M.; Rotem, A. Determination of Reinforcement Unbonding of Composites by a Vibration Technique. *J. Compos. Mater.* **2016**, *3*, 412–423. [CrossRef]
60. Kuriakose, V.M.; Sreehari, V.M. Experimental Investigation on the Enhancement of Vibration and Flutter Characteristics of Damaged Composite Plates Using Piezoelectric Patches. *Compos. Struct.* **2021**, *275*, 114518. [CrossRef]
61. Prasad Konka, H. Embedded Piezoelectric Fiber Composite Sensors for Applications in Composite Structures. Ph.D. Thesis, Louisiana State University and Agricultural and Mechanical College, Bâton-Rouge, LA, USA, 2011.
62. Konka, H.P.; Wahab, M.A.; Lian, K. On Mechanical Properties of Composite Sandwich Structures with Embedded Piezoelectric Fiber Composite Sensors. *J. Eng. Mater. Technol. Trans. ASME* **2012**, *134*, 011010. [CrossRef]
63. Kessler, S.S.; Spearing, S.M. In-Situ Sensor-Based Damage Detection of Composite Materials for Structural Health Monitoring. In Proceedings of the Collection of Technical Papers–AIAA/ASME/ASCE/AHS/ASC Structures, Structural Dynamics and Materials Conference, Denver, CO, USA, 22–25 April 2002; American Inst. Aeronautics and Astronautics Inc.: Reston, VA, USA, 2002; Volume 4, pp. 2706–2716.
64. De Medeiros, R.; Sartorato, M.; Tita, V.; De Medeiros, R.; Sartorato, M.; Vandepitte, D.; Tita, V. SHM of Composite Plates: Vibration Based Method by Using PZT Sensors. In Proceedings of the ISMA2014, Le Mans, France, 7–12 July 2014.
65. de Medeiros, R.; Sartorato, M.; Marques, F.D.; Tita, V.; De, R.; Murilo, M.; Flávio, S.; Marques, D.; Vandepitte, D. Vibration-Based Damage Identification Applied for Composite Plate: Experimental Analyses. In Proceedings of the COBEM 2013, Rio de Janeiro, Brazil, 3–7 November 2013.
66. Idriss, M.; El Mahi, A. Linear and Nonlinear Resonant Techniques for Characterizing Cyclic Fatigue Damage in Composite Laminate. *Compos. B Eng.* **2018**, *142*, 36–46. [CrossRef]
67. Idriss, M.; El Mahi, A.; El Guerjouma, R. Characterization of Sandwich Beams with Debonding by Linear and Nonlinear Vibration Method. *Compos. Struct.* **2015**, *120*, 200–207. [CrossRef]
68. El Mahi, A.; Idriss, M.; Assarar, M.; El Guerjouma, R.; Dazel, O. Effets de l'endommagement Sur Le Comportement Vibratoire Des Matériaux Sandwichs Endommagés. In Proceedings of the 19ème Congrès Français de Mécanique, Marseille, France, 24–28 August 2009.
69. Tracy, J.J.; Manager, S.; Pardoen, G.C. Effect of Delamination on the Natural Frequencies of Composite Laminates. *J. Compos. Mater.* **1989**, *23*, 1200–1251.
70. Ghoshal, A.; Chattopadhyay, A.; Schulz, M.J.; Thornburgh, R.; Waldron, K. Experimental Investigation of Damage Detection in Composite Material Structures Using a Laser Vibrometer and Piezoelectric Actuators. *J. Intell. Mater. Syst. Struct.* **2003**, *14*, 521–537. [CrossRef]
71. Okafor, A.C.; Chandrashekhara, K.; Jiang, Y.P. Delamination Prediction in Composite Beams with Built-in Piezoelectric Devices Using Modal Analysis and Neural Network. *Smart Mater. Struct.* **1996**, *5*, 338–347. [CrossRef]
72. Islam, A.S.; Craig, K.C. Damage Detection in Composite Structures Using Piezoelectric Materials. *Smart Mater. Struct.* **1994**, *3*, 318–328. [CrossRef]
73. Hou, J.P.; Jeronimidis, G. Vibration of Delaminated Thin Composite Plates. *Compos. Part A Appl. Sci. Manuf.* **1999**, *30*, 989–995. [CrossRef]
74. Lakhdar, M.; Mohammed, D.; Boudjemâa, L.; Rabiâ, A.; Bachir, M. Damages Detection in a Composite Structure by Vibration Analysis. *Energy Procedia* **2013**, *36*, 888–897. [CrossRef]
75. Siemens Company. Modal Tips: Roving Hammer versus Roving Accelerometer. Available online: https://community.sw.siemens.com/s/article/modal-tips-roving-hammer-versus-roving-accelerometer (accessed on 7 March 2022).
76. Pastor, M.; Binda, M.; Harčarik, T. Modal Assurance Criterion. *Procedia Eng.* **2012**, *48*, 543–548. [CrossRef]
77. Allemang, R.J. The Modal Assurance Criterion (MAC): Twenty Years of Use and Abuse. *Sound. Vib.* **2003**, *37*, 14–23.
78. Siemens Company. Modal Assurance Criterion (MAC). Available online: https://community.sw.siemens.com/s/article/modal-assurance-criterion-mac (accessed on 4 March 2022).
79. Patil, S.; Mallikarjuna Reddy, D. Damage Identification in Hemp Fiber (*Cannabis sativa*) Reinforced Composite Plates Using MAC and COMAC Correlation Methods: Experimental Study. *J. Nat. Fibers* **2020**, *19*, 1249–1264. [CrossRef]
80. dos Santos, F.L.M.; Peeters, B.; van der Auweraer, H.; Góes, L.C.S.; Desmet, W. Vibration-Based Damage Detection for a Composite Helicopter Main Rotor Blade. *Case Stud. Mech. Syst. Signal Process.* **2016**, *3*, 22–27. [CrossRef]
81. Pérez, M.A.; Gil, L.; Oller, S. Impact Damage Identification in Composite Laminates Using Vibration Testing. *Compos. Struct.* **2014**, *108*, 267–276. [CrossRef]
82. Herman, A.P.; Orifici, A.C.; Mouritz, A.P. Vibration Modal Analysis of Defects in Composite T-Stiffened Panels. *Compos. Struct.* **2013**, *104*, 34–42. [CrossRef]
83. Hu, H.; Wang, B.-T.; Su, J.-S. Application of Modal Analysis to Damage Detection in Composite Laminates. In Proceedings of the ESDA04, Manchester, UK, 19–22 July 2004.

84. Hu, H.; Wang, B.T.; Lee, C.H.; Su, J.S. Damage Detection of Surface Cracks in Composite Laminates Using Modal Analysis and Strain Energy Method. *Compos. Struct.* **2006**, *74*, 399–405. [CrossRef]
85. Qiao, P.; Lestari, W.; Shah, M.G.; Wang, J. Dynamics-Based Damage Detection of Composite Laminated Beams Using Contact and Noncontact Measurement Systems. *J. Compos. Mater.* **2007**, *41*, 1217–1252. [CrossRef]
86. Sampaio, R.P.C.; Maia, N.M.M.; Silva, J.M.M. Damage Detection Using the Frequency-Response-Function Curvature Method. *J. Sound. Vib.* **1999**, *226*, 1029–1042. [CrossRef]
87. Pandey, A.K.; Biswas, M.; Samman, M.M. Damage Detection from Changes in Curvature Mode Shapes. *J. Sound. Vib.* **1991**, *145*, 321–332. [CrossRef]
88. Radzieński, M.; Krawczuk, M.; Palacz, M. Improvement of Damage Detection Methods Based on Experimental Modal Parameters. *Mech. Syst. Signal Process.* **2011**, *25*, 2169–2190. [CrossRef]
89. Govindasamy, M.; Kamalakannan, G.; Kesavan, C.; Meenashisundaram, G.K. Damage Detection in Glass/Epoxy Laminated Composite Plates Using Modal Curvature for Structural Health Monitoring Applications. *J. Compos. Sci.* **2020**, *4*, 185. [CrossRef]
90. Lestari, W.; Qiao, P.; Hanagud, S. Curvature Mode Shape-Based Damage Assessment of Carbon/Epoxy Composite Beams. *J. Intell. Mater. Syst. Struct.* **2007**, *18*, 189–208. [CrossRef]
91. Hamey, C.S.; Lestari, W.; Qiao, P.; Song, G. Experimental Damage Identification of Carbon/Epoxy Composite Beams Using Curvature Mode Shapes. *Struct. Health Monit.* **2004**, *3*, 333–353. [CrossRef]
92. He, M.; Yang, T.; Du, Y. Nondestructive Identification of Composite Beams Damage Based on the Curvature Mode Difference. *Compos. Struct.* **2017**, *176*, 178–186. [CrossRef]
93. Mehdizadeh, M. Curvature Mode Shape Analyses of Damage in Structures. Ph.D. Thesis, School of Aerospace, Mechanical & Manufacturing Engineering College of Science, Engineering and Technology, Bundoora, Australia, 2009.
94. Sazonov, E.; Klinkhachorn, P. Optimal Spatial Sampling Interval for Damage Detection by Curvature or Strain Energy Mode Shapes. *J. Sound. Vib.* **2005**, *285*, 783–801. [CrossRef]
95. Cha, Y.J.; Buyukozturk, O. Structural Damage Detection Using Modal Strain Energy and Hybrid Multiobjective Optimization. *Comput. Aided Civ. Infrastruct. Eng.* **2015**, *30*, 347–358. [CrossRef]
96. Eraky, A.; Anwar, A.M.; Saad, A.; Abdo, A. Damage Detection of Flexural Structural Systems Using Damage Index Method—Experimental Approach. *Alex. Eng. J.* **2015**, *54*, 497–507. [CrossRef]
97. Wang, S.; Xu, M. Modal Strain Energy-Based Structural Damage Identification: A Review and Comparative Study. *Struct. Eng. Int.* **2019**, *29*, 234–248. [CrossRef]
98. Hu, H.; Wang, J. Damage Detection of a Woven Fabric Composite Laminate Using a Modal Strain Energy Method. *Eng. Struct.* **2009**, *31*, 1042–1055. [CrossRef]
99. Hu, H.; Lee, C.H.; Wu, C.B.; Lu, W.J. Detection of Matrix Cracks in Composite Laminates by Using the Modal Strain Energy Method. *Mech. Compos. Mater.* **2010**, *46*, 117–132. [CrossRef]
100. dos Santos, F.L.M.; Peeters, B.; van der Auweraer, H.; Góes, L.C.S. Modal Strain Energy Based Damage Detection Applied to a Full Scale Composite Helicopter Blade. *Key Eng. Mater.* **2013**, *569–570*, 457–464.
101. Kumar, M.; Shenoi, R.A.; Cox, S.J. Experimental Validation of Modal Strain Energies Based Damage Identification Method for a Composite Sandwich Beam. *Compos. Sci. Technol.* **2009**, *69*, 1635–1643. [CrossRef]
102. Meng, F.; Yu, J.; Alaluf, D.; Mokrani, B.; Preumont, A. Modal Analysis and Damage Detection for Suspension Bridges: A Numerical and Experimental Investigation. *Smart Struct. Syst.* **2019**, *23*, 15–29.
103. Yang, J.S.; da Liu, Z.; Schmidt, R.; Schröder, K.U.; Ma, L.; Wu, L.Z. Vibration-Based Damage Diagnosis of Composite Sandwich Panels with Bi-Directional Corrugated Lattice Cores. *Compos. Part. A Appl. Sci. Manuf.* **2020**, *131*, 105781. [CrossRef]
104. Cao, M.S.; Sha, G.G.; Gao, Y.F.; Ostachowicz, W. Structural Damage Identification Using Damping: A Compendium of Uses and Features. *Smart Mater. Struct.* **2017**, *26*, 043001. [CrossRef]
105. Inman, D.J. *Engineering Vibration*; Pearson Education Limited: London, UK, 1994; ISBN 978-0-13-287169-3.
106. Slavič, J.; Simonovski, I.; Boltežar, M. Damping Identification Using a Continuous Wavelet Transform: Application to Real Data. *J. Sound. Vib.* **2003**, *262*, 291–307. [CrossRef]
107. Montalvão, D.; Ribeiro, A.M.R.; Duarte-Silva, J. A Method for the Localization of Damage in a CFRP Plate Using Damping. *Mech. Syst. Signal Process.* **2009**, *23*, 1846–1854. [CrossRef]
108. Montalvão, D.; Ribeiro, A.M.R.; Duarte-Silva, J.A.B. Experimental Assessment of a Modal-Based Multi-Parameter Method for Locating Damage in Composite Laminates. *Exp. Mech.* **2011**, *51*, 1473–1488. [CrossRef]
109. Montalvão, D.; Karanatsis, D.; Ribeiro, A.M.; Arina, J.; Baxter, R. An Experimental Study on the Evolution of Modal Damping with Damage in Carbon Fiber Laminates. *J. Compos. Mater.* **2015**, *49*, 2403–2413. [CrossRef]
110. Kessler, S.S.; Spearing, S.M.; Atalla, M.J.; Cesnik, C.E.S.; Soutis, C. Damage Detection in Composite Materials Using Frequency Response Methods. *Compos. Part B* **2002**, *33*, 87–95. [CrossRef]
111. Sampaio, R.P.C.; Maia, N.M.M.; Silva, J.M.M. The Frequency Domain Assurance Criterion as a Tool for Damage Detection. *Key Eng. Mater.* **2003**, *245–246*, 69–76. [CrossRef]
112. Chen, A. Frequency Response Assurance Criterion and Applications to Model Correlation of Body Structures. *SAE Tech. Pap.* **2003**. [CrossRef]

113. de Medeiros, R. Development of a Criterion for Predicting Residual Strength of Composite Structures Damaged by Impact Loading. Ph.D. Thesis, Mechanical Engineering, University of Sao Paulo–USP Sao Carlos School of Engineering, Sao Paulo, Brazil, 2016.
114. Chesné, S.; Deraemaeker, A. Damage Localization Using Transmissibility Functions: A Critical Review. *Mech. Syst. Signal Process.* **2013**, *38*, 569–584. [CrossRef]
115. Zhang, H.; Schulz, M.J.; Ferguson, F.; Pai, P.F. Structural Health Monitoring Using Transmittance Functions. *Mech. Syst. Signal Process.* **1999**, *13*, 765–787. [CrossRef]
116. Sundaresan, M.; Ferguson, F.; Pai, P.; Sundaresan, M.J.; Schulz, M.J.; Hill, J.; Wheater, E.A.; Ferguson, F.; Pai, P.F. Damage Detection on a Wind Turbine Blade Section. In Proceedings of the International Society for Optical Engineering, San Jose, CA, USA, 26–28 January 1999.
117. Poulimenos, A.G.; Sakellariou, J.S. A Transmittance-Based Methodology for Damage Detection under Uncertainty: An Application to a Set of Composite Beams with Manufacturing Variability Subject to Impact Damage and Varying Operating Conditions. *Struct. Health Monit.* **2019**, *18*, 318–333. [CrossRef]
118. Liu, C.-L. A Tutorial of the Wavelet Transform. *NTUEE* **2010**, *21*, 22.
119. Yan, Y.J.; Yam, L.H. Detection of Delamination Damage in Composite Plates Using Energy Spectrum of Structural Dynamic Responses Decomposed by Wavelet Analysis. *Comput. Struct.* **2004**, *82*, 347–358. [CrossRef]
120. Singh, A.K. Detection of Defects in Composite Laminates with Vibro-Ultrasonic Methods. Ph.D. Thesis, National University of Singapore, Singapore, 2019.
121. Andreaus, U.; Baragatti, P. Experimental Damage Detection of Cracked Beams by Using Nonlinear Characteristics of Forced Response. *Mech. Syst. Signal Process.* **2012**, *31*, 382–404. [CrossRef]
122. Dolbachian, L.; Harizi, W.; Aboura, Z. Structural Health Monitoring (SHM) Study of Polymer Matrix Composite (PMC) Materials Using Nonlinear Vibration Methods Based on Embedded Piezoelectric Transducers. *Sensors* **2023**, *23*, 3677. [CrossRef]
123. Andreades, C.; Ciampa, F. CFRP Composites with Embedded PZT Transducers for Nonlinear Ultrasonic Inspection of Space Structures. In Proceedings of the EWSHM2018, Manchester, UK, 10–13 July 2018.
124. Andreades, C.; Malfense Fierro, G.P.; Meo, M. A Nonlinear Ultrasonic SHM Method for Impact Damage Localisation in Composite Panels Using a Sparse Array of Piezoelectric PZT Transducers. *Ultrasonics* **2020**, *108*, 106181. [CrossRef]
125. Polimeno, U.; Meo, M.; Almond, D.P. Smart Nonlinear Acoustic Based Structural Health Monitoring System. *Adv. Sci. Technol.* **2008**, *56*, 426–434. [CrossRef]
126. Loi, G.; Porcu, M.C.; Aymerich, F. Impact Damage Detection in Composite Beams by Analysis of Non-Linearity under Pulse Excitation. *J. Compos. Sci.* **2021**, *5*, 39. [CrossRef]
127. Ooijevaar, T.H.; Rogge, M.D.; Loendersloot, R.; Warnet, L.L.; Akkerman, R.; Tinga, T. Nonlinear Dynamic Behavior of an Impact Damaged Composite Skin-Stiffener Structure. *J. Sound. Vib.* **2015**, *353*, 243–258. [CrossRef]
128. Wei, L.; Chen, J. Far-End Delamination Characterization of CFRP Laminates Using Nonlinear Ultrasonic Spectra of Scaling Subtracted Vibration Response. *Compos. Commun.* **2024**, *45*, 101811. [CrossRef]
129. Meo, M.; Polimeno, U.; Zumpano, G. Detecting Damage in Composite Material Using Nonlinear Elastic Wave Spectroscopy Methods. *Appl. Compos. Mater.* **2008**, *15*, 115–126. [CrossRef]
130. Polimeno, U.; Meo, M. Understanding the Effect of Boundary Conditions on Damage Identification Process When Using Nonlinear Elastic Wave Spectroscopy Methods. *Int. J. Non Linear Mech.* **2008**, *43*, 187. [CrossRef]
131. Bentahar, M. Nonlinear Acoustics: Application to Ultrasonic Characterisation of Damage in Heterogeneous Materials and Remaining Life Determination. Ph.D. Thesis, INSA Lyon, Lyon, France, 2005.
132. Wei, Q.; Zhu, L.; Zhu, J.; Zhuo, L.; Hao, W.; Xie, W. Characterization of Impact Fatigue Damage in CFRP Composites Using Nonlinear Acoustic Resonance Method. *Compos. Struct.* **2020**, *253*, 112804. [CrossRef]
133. van den Abeele, K.E.A.; Sutin, A.; Carmeliet, J.; Johnson, P.A. Micro-Damage Diagnostics Using Nonlinear Elastic Wave Spectroscopy (NEWS). *NDT E Int.* **2001**, *34*, 239–248. [CrossRef]
134. Novak, A.; Bentahar, M.; Tournat, V.; el Guerjouma, R.; Simon, L. Nonlinear Acoustic Characterization of Micro-Damaged Materials through Higher Harmonic Resonance Analysis. *NDT E Int.* **2012**, *45*, 1–8. [CrossRef]
135. Haggui, M.; Jendli, Z.; El Mahi, A.; Akrout, A.; Haddar, M. Damage Analysis in Flax/Elium Composite Using Linear and Nonlinear Resonance Techniques. *J. Vib. Eng. Technol.* **2023**. [CrossRef]
136. Pieczonka, L.; Klepka, A.; Martowicz, A.; Staszewski, W.J. Nonlinear Vibroacoustic Wave Modulations for Structural Damage Detection: An Overview. *Opt. Eng.* **2015**, *55*, 011005. [CrossRef]
137. Andreades, C.; Malfense Fierro, G.P.; Meo, M.; Ciampa, F. Nonlinear Ultrasonic Inspection of Smart Carbon Fibre Reinforced Plastic Composites with Embedded Piezoelectric Lead Zirconate Titanate Transducers for Space Applications. *J. Intell. Mater. Syst. Struct.* **2019**, *30*, 2995–3007. [CrossRef]
138. Klepka, A.; Pieczonka, L.; Staszewski, W.J.; Aymerich, F. Impact Damage Detection in Laminated Composites by Non-Linear Vibro-Acoustic Wave Modulations. *Compos. B Eng.* **2014**, *65*, 99–108. [CrossRef]
139. Adebahr, W.; Solodov, I.; Rahammer, M.; Gulnizkij, N.; Kreutzbruck, M. Local Defect Resonance for Sensitive Non-Destructive Testing. In Proceedings of the AIP Conference Proceedings, Liptovsky Jan, Slovakia, 9–11 April 2014; American Institute of Physics Inc.: Melville, NY, USA, 10 February 2016; Volume 1706.

140. Solodov, I.; Bai, J.; Bekgulyan, S.; Busse, G. A Local Defect Resonance to Enhance Acoustic Wave-Defect Interaction in Ultrasonic Nondestructive Evaluation. *Appl. Phys. Lett.* **2011**, *99*, 211911. [CrossRef]
141. Solodov, I.; Bai, J.; Bekgulyan, S.; Busse, G. A Local Defect Resonance to Enhance Wave-Defect Interaction in Nonlinear Spectroscopy and Ultrasonic Thermography. In Proceedings of the World Conference on Nondestructive Testing, Durban, South Africa, 16–20 April 2012.
142. Aymerich, F.; Staszewski, W.J. Impact Damage Detection in Composite Laminates Using Nonlinear Acoustics. *Compos. Part A Appl. Sci. Manuf.* **2010**, *41*, 1084–1092. [CrossRef]
143. Aymerich, F.; Staszewski, W.J. Experimental Study of Impact-Damage Detection in Composite Laminates Using a Cross-Modulation Vibro-Acoustic Technique. *Struct. Health Monit.* **2010**, *9*, 541–553. [CrossRef]
144. Ooijevaar, T.H.; Loendersloot, R.; Rogge, M.D.; Akkerman, R.; Tinga, T. Vibro-Acoustic Modulation Based Damage Identification in a Composite Skin-Stiffener Structure. *Struct. Health Monit.* **2016**, *15*, 458–472. [CrossRef]
145. Ooijevaar, T.H.; Loendersloot, R.; Warnet, L.L.; de Boer, A.; Akkerman, R. Vibration Based Structural Health Monitoring of a Composite T-Beam. *Compos. Struct.* **2010**, *92*, 2007–2015. [CrossRef]
146. Chen, B.Y.; Soh, S.K.; Lee, H.P.; Tay, T.E.; Tan, V.B.C. A Vibro-Acoustic Modulation Method for the Detection of Delamination and Kissing Bond in Composites. *J. Compos. Mater.* **2016**, *50*, 3089–3104. [CrossRef]
147. Prevorovsky, Z.; Krofta, J.; Kober, J.; Chlada, M.; Kirchner, A. Non-Linear Ultrasonic Spectroscopy of 3D Printed Metallic Samples. *Insight Non-Destr. Test. Cond. Monit.* **2019**, *61*, 157–161. [CrossRef]
148. Loi, G.; Uras, N.; Porcu, M.C.; Aymerich, F. Damage Detection in Composite Materials by Flexural Dynamic Excitation and Accelerometer-Based Acquisition. *IOP Conf. Ser. Mater. Sci. Eng.* **2022**, *1214*, 012007. [CrossRef]
149. Kim, S.; Adams, D.E.; Sohn, H.; Rodriguez-Rivera, G.; Myrent, N.; Bond, R.; Vitek, J.; Carr, S.; Grama, A.; Meyer, J.J. Crack Detection Technique for Operating Wind Turbine Blades Using Vibro-Acoustic Modulation. *Struct. Health Monit.* **2014**, *13*, 660–670. [CrossRef]
150. Willmann, E.; Boll, B.; Mikaelyan, G.; Wittich, H.; Meißner, R.H.; Fiedler, B. Vibro-Acoustic Modulation Based Measurements in CFRP Laminates for Damage Detection in Open-Hole Structures. *Compos. Commun.* **2023**, *42*, 101659. [CrossRef]
151. Ruiz, D.V.; de Bragança, C.S.C.; Poncetti, B.L.; Bittencourt, T.N.; Futai, M.M. Vibration-Based Structural Damage Detection Strategy Using FRFs and Machine Learning Classifiers. *Structures* **2024**, *59*, 105753. [CrossRef]